

Theory of adiabatic spinodal decomposition in binary fluids

James P. Donley

Valence4 Technologies, Arlington, VA 22202*

(Dated: September 29, 2018)

A generalization of the Kawasaki, Ohta/Langer, Bar-on, Miller theory of early-stage spinodal decomposition in a near-critical binary fluid is presented. The theory accounts for experimental scenarios in which the system is quenched abruptly by changing the pressure and the subsequent phase separation occurs adiabatically. Equations of motion for the system volume and effective temperature are derived. It is shown that for this case the non-equilibrium decomposition process is well approximated as one of constant entropy, that is, as thermodynamically reversible. This generalized theory is compared, with no adjustable parameters, to experimental light scattering data of Bailey and Cannell. It is found that this adiabatic theory is in satisfactory agreement with this data throughout the early stage. It is also shown that at later times the Kawasaki and Ohta theory predicts that the peak wavevector q_m of the structure factor scales with time as t^{-a_q} , with $a_q \approx 0.46$. The equilibrium static critical properties of the Langer, Bar-on, Miller theory are also examined, this discussion serving to justify some approximations in the adiabatic theory.

I. INTRODUCTION

Spinodal decomposition is the process of phase separation of a thermodynamically unstable mixture.[1–4] It and its complement, nucleation, are two of the most common mechanisms of phase transformation for systems governed by a conserved order parameter. They also are exploited in many commercial processes for creating alloy materials.

In decomposition, experiments typically measure the intensity $I(k, t)$ of X-rays, neutrons or light scattered by the mixture at various momentum transfer wavevectors $k = |\mathbf{k}|$ and times t . Information about the state of the mixture, e.g., metal alloy, polymer blend, composite glass or binary fluid, is obtained by relating $I(k, t)$ to the structure factor $\hat{S}(k, t)$, which is the Fourier transform of the density-density correlation function. To initiate decomposition, a uniform mixture in equilibrium is quenched into the middle-part of the two-phase coexistence region, usually by cooling the sample. After the quench a ring of scattered radiation surrounding the incident beam of the radiation probe appears. The peak intensity of the ring corresponds initially to a wavevector $k_m \approx 1/\xi$, where ξ is the correlation length of the equilibrium coexisting phases (assumed to be the same for both) at the quenched temperature. Over time this ring shrinks, implying that the precipitate is coarsening. At late times k_m has been shown to vary as a power of the time t , $k_m \sim t^{-a_q}$, and $\hat{S}(k, t)$ to reduce to a scaling form. This late stage scaling is thought to be due to the formation of growing domains of average size $L \sim 1/k_m$. These domains have well-defined interfaces of thickness ξ and the composition inside the domains is near the coexistence values of the mixture.

Decomposition was studied initially for systems in which phase separation is driven by single particle diffusion, such as metal alloys. The first theories of the

early stage of decomposition in such substances were due to Cahn[1] and Cook[5], and later Langer, Bar-on and Miller (LBM)[6]. Experimental tests of these theories have not been entirely unambiguous though. For metal alloys, lattice mismatch of the two components can cause stresses to build during unmixing, which slows the rate of decomposition. These strains can be minimized by matching the lattice constants of the individual components [7], or avoided entirely by examining unmixing in liquids [8, 9]. In liquids though, unmixing is greatly accelerated by advection. Kawasaki and Ohta (KO) extended the LBM theory to binary liquids by incorporating these hydrodynamic effects.[10]

A careful set of experiments to test this KO theory was done by Bailey and Cannell (BC) using 3-methylpentane and nitroethane (3MP+NE) in the critical region.[11] The critical equilibrium properties of 3MP+NE have been well characterized. Further, the components of this binary liquid have very similar indices of refraction, which minimizes multiple scattering effects during decomposition. Since all the parameters of the KO-LBM theory can be obtained from equilibrium measurements, a clear comparison with the theory would seem to be possible. However, as BC have discussed, their experiments violated an almost universal theoretical assumption for this class of non-equilibrium phenomena, namely, that the temperature is a control parameter. Rather, the quenches occurred by rapidly decreasing the pressure and then holding it constant during the decomposition. On the timescale of their experiments, no heat from the container walls was able to reach the portion of the liquid being probed; thus the decomposition occurred adiabatically rather than isothermally. The problem with controlling only the pressure is that unmixing releases heat (being exothermic for most simple liquids), and so the temperature of the sample will be increasing over time. Theories of dynamic critical phenomena and the KO theory itself predict that the characteristic relaxation time of a binary liquid scales as $\xi^{3+z_\eta} \sim |\epsilon|^{-1.94}$, where $\epsilon = T/T_c - 1$ is the reduced temperature, with

* jdonley@valence4.com

T and T_c being the absolute and critical temperature, respectively.[12] The experiments of BC were done at absolute reduced temperatures around 10^{-5} , and so small changes in T could cause large changes in the relaxation time making comparison with theory potentially troublesome. More fundamentally though, what does one mean by “temperature” when a system is driven so far from equilibrium?

This paper has two purposes. First, it gives an answer to this and some related questions, and generalizes the KO-LBM theory to adiabatic decomposition. Second, it compares quantitatively this generalized theory to the BC experiments.

The problem of decomposition under adiabatic conditions was first addressed in [13]. The concepts and approach described in that work are further explored in the present one.

The paper is organized as follows. In Sec. II the basic theory of adiabatic decomposition is presented. The product of the theory is an equation of motion for the effective system temperature. Then, the isothermal coarse-grained free energy used in KO and LBM is generalized to describe systems for which the temperature is changing. In Sec. III the hydrodynamic KO theory for the equation of motion of the structure factor is described, one reason being to show how the temperature dependence of the theory arises. The equilibrium form of the LBM theory is also discussed, it being used to compute initial conditions for the kinetic theory. In Sec. IV the temperature and structure factor kinetic equations, along with the equilibrium equations for the structure factor, are scaled. Then, the scheme used here to solve them numerically is discussed. In Sec. V the parameters in the temperature dependent coarse-grained free energy are determined using the equilibrium LBM theory. The predictions of the equilibrium LBM theory in the critical region are then discussed, primarily to show in what regions of the phase diagram the theory can be used to give accurate initial conditions, and properly describe the un-mixing process in a thermodynamic sense. In Sec. VI general predictions of the adiabatic and isothermal kinetic theories are presented, including the behavior of the KO theory at late times, far beyond its supposed regime of validity. The adiabatic and isothermal theories are then compared quantitatively with the BC experiments. Finally, in Sec. VII the paper is summarized and directions for further work are discussed.

II. ADIABATIC DECOMPOSITION

In this section a theory of adiabatic decomposition in a binary substance is presented. The theory generalizes any isothermal, statistical theory of decomposition, such as KO or LBM.

In what follows, the equilibrium properties of critical binary fluids will be referred to justify some theoretical approximations. Table I below contains equilibrium data

of 3MP+NE relevant to the theory here. Table II below contains relevant critical exponent values and amplitude relations. In this work, the critical point for a given pressure P is denoted by the concentration c_c and temperature T_c . As mentioned above, the reduced temperature $\epsilon = T/T_c - 1$. For 3MP+NE at the pressures of interest, T_c varies linearly with pressure, so $\frac{dT_c}{dP}$ is a constant.[14] In the critical region, the miscibility gap has the scaling form $\Delta c = 2B|\epsilon|^\beta$; the correlation length $\xi = \xi_0^\pm |\epsilon|^{-\nu}$; and the susceptibility $\chi = \Gamma^\pm |\epsilon|^{-\gamma}$, with β, γ and ν being critical exponents and B, ξ_0^\pm and Γ^\pm being critical amplitudes. Here, “+” refers to a one-phase value obtained on the critical isobar above T_c , while “-” refers to a two-phase coexistence value below T_c . The quantities c_c, B, ξ_0, Γ and any other critical amplitude mentioned in this text have either been shown experimentally to be, or are assumed to be constant over the pressures of experimental interest.[14]

A. Basic Theory

The essence of the theory here is to exploit how one constructs the coarse-grained free energy \mathcal{F} used in previous theories of decomposition.[23] It is defined as follows.[24] Consider a binary mixture of A and B -type molecules in strong contact with an external reservoir at

TABLE I. Equilibrium one-phase ($T > T_c$) data of an on-critical mixture of 3MP+NE relevant to the present work. All units are MKS.

Parameter		Ref.
Critical Temperature	$T_c = 300^\circ\text{K}$	[14]
	$\frac{dT_c}{dP} = 3.497 \times 10^{-8} \text{ K/Pa}$	[15]
Critical Mass Density	$\rho_c = 7.92 \times 10^2 \text{ kg/m}^3$	[16]
Correlation Length	$\xi = \xi_0^+ \epsilon ^{-\nu}$	
	$\xi_0^+ = 2.207 \times 10^{-10} \text{ m}$ with $\nu = 0.632$	[15]
Hydrodynamic Shear Viscosity	$\eta_s = \bar{\eta}(Q_0\xi)^{z_\eta}$	
	$\bar{\eta} = 3.76 \times 10^{-4} \text{ Pa-sec}$	[17]
	$Q_0 = 1.4 \times 10^8 \text{ m}^{-1}$	[18]
	$z_\eta = 0.063$	[18]
Isobaric Heat Capacity	$C_p = C_0^+ \epsilon ^{-\alpha} + C_b$	
	$C_0^+ = 2.881 \times 10^2 \text{ J/(K-kg)}$	[15]
	$C_b = 1.7074 \times 10^3 \text{ J/(K-kg)}$	[15]
	with $\alpha = 0.105$	
Thermal Expansion Coefficient	$\alpha_p = A_0^+ \epsilon ^{-\alpha} + A_b$	
	$A_0^+ = 2.6597 \times 10^{-5} \text{ K}^{-1}$	[15]
	$A_b = 1.284 \times 10^{-3} \text{ K}^{-1}$	[15]
	with $\alpha = 0.105$	
Adiabatic Compressibility	$K_s \approx 1.07 \times 10^{-9} \text{ Pa}$	[19]

temperature T . Let $c(\mathbf{r})$ be the concentration of A -type molecules in a cell of size a^3 centered at position \mathbf{r} . The cell size is mesoscopic on the order of the equilibrium correlation length ξ , which for mixtures in the critical region can be hundreds or even thousands of angstroms. The coarse-grained free energy $\mathcal{F} \equiv \mathcal{F}[c]$, is a functional of the concentration field $c(\mathbf{r})$. In mean-field theories a change in $\mathcal{F}[c]$ due to a change in the concentration at some point \mathbf{r} acts as a local thermodynamic driving force or chemical potential $\mu(\mathbf{r})$. Gradients in $\mu(\mathbf{r})$ in turn cause mass diffusion.

The coarse-grained free energy is constructed by fixing the value of $c(\mathbf{r})$ in each cell and performing the partition sum over all states of the system consistent with the configuration $[c]$. Let the microscopic Hamiltonian be H , then

$$\exp\left(-\frac{\mathcal{F}[c] + F_r}{k_B T}\right) = \sum_{\substack{\text{states} \\ \text{consistent} \\ \text{with}[c]}} \exp\left(-\frac{H}{k_B T}\right), \quad (\text{II.1})$$

where k_B is Boltzmann's constant. The coarse-grained free energy \mathcal{F} then describes the properties of all concentration modes of wavenumber k less than some cut-off $\Lambda \sim 1/a$. The quantity F_r is the part of the total equilibrium free energy that is independent of the configuration $[c]$. For example, it is assumed that F_r contains all vibrational degrees of freedom, which give the dominant contribution to a liquid's entropy. In addition, the short wavelength concentration modes ($k > \Lambda$) contribute to F_r , but they also contribute to \mathcal{F} by renormalizing its coefficients. Because the long wavelength concentration modes don't contribute to F_r , F_r is an analytic function of $T - T_c$. [25]

Since the interest here is in the kinetics of phase separation, in integrating out these degrees of freedom it is assumed that they relax very quickly compared to the modes described by $[c]$. That is, the modes in F_r are able to equilibrate between any characteristic change in $[c]$. Note that the separation of the partial free energy

TABLE II. Theoretical critical exponent and amplitude relations for binary fluids relevant to the present work.

Exponent	Value	Reference
ν	0.632	[20]
γ	1.2395	[20]
α	0.105	[20]
Amplitude Ratio	Value	Reference
$\frac{\Gamma^+}{\Gamma^-}$	4.95	[21]
$\frac{\xi_0^+}{\xi_0^-}$	1.96	[21]
$\frac{C_0^+}{C_0^-}$	0.523	[21]
$\frac{T_c A_0^+}{\rho_c C_0^+}$	$\frac{dT_c}{dP}$	[22]
$\frac{\alpha \rho_c C_0^+}{k_B} \frac{\Gamma^+}{B^2}$	0.0581	[21]
$\xi_0^+ \left(\frac{\alpha \rho_c C_0^+}{k_B}\right)^{1/3}$	0.265	[21]

into two terms \mathcal{F} and F_r implies weak coupling between those degrees of freedom that contribute to F_r and the configuration $[c]$.

Such a separation matters little to the isothermal theory as F_r is ignored. However, what if the system were not in strong contact with an external bath? Would it be possible to let the degrees of freedom that have been integrated out act as a thermal reservoir for the long wavelength modes in this case?

1. Closed System

To implement this idea and clarify the concepts, it is helpful to look first at a system that is closed, i.e. has a fixed total energy E_t and fixed volume V .

First, does the heat released during decomposition cause non-uniformities in the temperature T or pressure P ? The speed of sound is clearly faster than any diffusion process being considered, so P can be easily approximated as uniform. For decomposition it is expected that if any non-uniformities in temperature occur, they occur over a wavelength $\lambda \sim 1/q_m \geq \xi$, where q_m is the wavevector of the peak scattering intensity and is a measure of the size of the phase separating regions. Thus, the characteristic time τ_T for heat to diffuse across a distance λ must be compared with the characteristic relaxation time τ_c of a concentration mode of size λ . It can be shown that, for a typical binary fluid, $\frac{\tau_T}{\tau_c} = \frac{D_c}{D_T} \sim 10^{-4} \ll 1$, and so T can safely assumed to also be uniform.

Now, for the closed system, the relevant "free energy" is the entropy S . In analogy with the definition for \mathcal{F} and following Boltzmann, define

$$S([c], E_t) = k_B \ln \left[\sum_{\substack{\text{states} \\ \text{consistent} \\ \text{with}[c]}} \delta(H - E_t) \right], \quad (\text{II.2})$$

as the entropy of a system with a fixed configuration $[c]$ and total energy E_t . Here, $\delta(x)$ is the Dirac "delta" function at point x .

However, for the approximations to follow the interest is still with \mathcal{F} . To construct \mathcal{F} , define the partition function

$$\begin{aligned} Z &= \sum_{\substack{\text{states} \\ \text{consistent} \\ \text{with}[c]}} \exp(-\beta H) \\ &= \int dE' \exp(-\beta E') \Gamma(E', [c]), \end{aligned} \quad (\text{II.3})$$

where β is a parameter to be determined, and $\Gamma([c], E') = \exp(S([c], E')/k_B)$ is the number of accessible states of the system with an energy E' and coarse-grained configuration $[c]$. Expanding S about E_t it is found that, for the case in which Γ is a macroscopic number, S is related to Z by

$$S([c], E_t) - k_B \beta E_t = k_B \ln Z, \quad (\text{II.4})$$

with

$$k_B\beta = \left(\frac{\partial S}{\partial E_t}\right)_{V,[c]}. \quad (\text{II.5})$$

Now, as in the isothermal case, assume weak coupling so that S can be written as

$$S([c], E_t) = \mathcal{S}[c] + S_r, \quad (\text{II.6})$$

where S_r is the part of the entropy independent of the configuration $[c]$. Let the energy associated with S_r and $\mathcal{S}[c]$ be E_r and $\mathcal{E}[c]$, respectively. Then,

$$E_t = \mathcal{E}[c] + E_r. \quad (\text{II.7})$$

If the concentration field $[c]$ is held fixed, then so will be $\mathcal{S}[c]$ and $\mathcal{E}[c]$; thus,

$$\left(\frac{\partial S}{\partial E_t}\right)_{V,[c]} = \left(\frac{\partial S_r}{\partial E_r}\right)_V \equiv \frac{1}{T_r}. \quad (\text{II.8})$$

Combining Eqs. (II.3)-(II.8) then gives

$$\exp\left(-\frac{\mathcal{F}[c] + F_r}{k_B T_r}\right) = \sum_{\substack{\text{states} \\ \text{consistent} \\ \text{with}[c]}} \exp\left(-\frac{H}{k_B T_r}\right), \quad (\text{II.9})$$

where the coarse-grained free energy

$$\mathcal{F} = \mathcal{E} - T_r \mathcal{S}, \quad (\text{II.10})$$

and

$$F_r = E_r - T_r S_r. \quad (\text{II.11})$$

Comparing Eqs. (II.1) and (II.9) it can be seen for this closed system that the degrees of freedom contributing to F_r act explicitly as a reservoir for the concentration modes described by \mathcal{F} . Note though that because the total energy E_t is constrained, T_r through Eq. (II.7) is not a constant, but an implicit function of the concentration field $[c]$.

For the remainder of this work, the degrees of freedom that contribute to F_r will be called the reservoir, and those that are described by the concentration field $[c]$ and contribute to $\mathcal{F}[c]$ will be called the slow modes.

Now, is T_r related to any measurable temperature T ? An average reservoir temperature, " $\langle T_r \rangle$ ", can be obtained by computing the average coarse-grained energy $\langle \mathcal{E}[c] \rangle$ using $\rho([c], E_t)$, which is the probability density that the system is in a configuration $[c]$ with total system energy E_t . That is, with $\langle \mathcal{E}[c] \rangle$, the average reservoir energy is $E_t - \langle \mathcal{E}[c] \rangle$, so an average T_r is known. It can be shown that in equilibrium, $\langle T_r \rangle$ is equal to the average system temperature $T = \left(\frac{\partial E_t}{\partial S_t}\right)_V$, where S_t is the total equilibrium entropy.[26] When the system is out of equilibrium, the relation of $\langle T_r \rangle$ to the system temperature is unclear - assuming the latter can even be defined in a consistent manner. However, as will be seen below,

such a relation is not necessary to determine the time evolution of the concentration field.

For a closed system, the equilibration process is as follows. The system is prepared in some non-equilibrium state with reservoir energy E_r and coarse-grained configuration $[c]$ (and thus energy $\mathcal{E}[c]$). The system is then released and the configuration $[c]$ evolves. The evolution is driven by $\mathcal{F}[c]$, which is a function of the reservoir temperature T_r . As the $[c]$ changes, the coarse-grained energy $\mathcal{E}[c]$ changes, and, because the total energy is constant, the reservoir energy E_r changes. A change in E_r implies a change in T_r , and this change in T_r in turn affects the evolution of the $[c]$ and so on. The system eventually settles down into a state that maximizes the total entropy.

With the ideas above, an equation of motion for $\rho([c], E_t)$ for the case in which mass transfer is dominated by single particle diffusion (the solid model[27]) can be derived, but the coupling between the reservoir and slow modes makes this equation not too useful.

A simpler approach is as follows. The primary concern here is with average temperature changes associated with the decomposition process. The idea then is to let the average reservoir temperature $\langle T_r \rangle = T$ play the role of a pseudo control parameter, the thermodynamic driving force be $\mathcal{F} = \mathcal{E} - T\mathcal{S}$, and derive a separate equation of motion for T . In this way the same equation for $\rho([c], t)$ that has been used to describe isothermal decomposition will be used, but any temperature dependent parameter will now vary in time.

The time evolution of T can be obtained using energy conservation. For the closed system this is easily done. Eq. (II.7) obviously also holds for averages, so for a differential change

$$d\langle E_t \rangle = dE_r + d\langle \mathcal{E}[c] \rangle = 0. \quad (\text{II.12})$$

The reservoir energy is an equilibrium thermodynamic function so

$$dE_r = C_{Vr} dT, \quad (\text{II.13})$$

where $C_{Vr} = \left(\frac{\partial E_r}{\partial T}\right)_V$ is the reservoir heat capacity at constant volume. Also,

$$d\langle \mathcal{E}[c] \rangle = \frac{\partial \langle \mathcal{E}[c] \rangle}{\partial t} dt, \quad (\text{II.14})$$

where the partial time derivative of the average is defined by

$$\frac{\partial \langle \mathcal{E}[c] \rangle}{\partial t} \equiv \int d[c] \mathcal{E}[c] \frac{\partial \rho([c], t)}{\partial t}, \quad (\text{II.15})$$

with $\int d[c]$ denoting an integral over the space of possible concentration fields. Note that the term $\langle \frac{\partial \mathcal{E}[c]}{\partial T} \rangle dT$ does not appear in Eq.(II.14) since in the above construction of $\mathcal{F}[c]$, $\mathcal{E}[c]$ is independent of temperature. Combining Eqs. (II.12-II.14) gives:

$$\frac{dT}{dt} = -\frac{1}{C_{Vr}} \frac{\partial \langle \mathcal{E}[c] \rangle}{\partial t}. \quad (\text{II.16})$$

Since the free energies are additive,

$$C_{Vr} = C_V - C_{Vcg}, \quad (\text{II.17})$$

where C_V is the equilibrium heat capacity of the total system, and C_{Vcg} is the contribution to C_V from the slow modes. C_V can be obtained from experiment and C_{Vcg} can be calculated once $\mathcal{F}[c]$ is defined:

$$C_{Vcg} = -T \left(\frac{\partial^2 F_{cg}}{\partial T^2} \right)_V, \quad (\text{II.18})$$

where $F_{cg} = -k_B T \ln Z$ is the portion of the total system Helmholtz free energy from the slow modes, with the partition function $Z = \int d[c] \exp(-\frac{\mathcal{F}[c]}{k_B T})$.

2. Adiabatic System

These same ideas will now be applied to adiabatic decomposition. In this case there is of course no heat flow between the system and the outside world, and the pressure P instead of T will be a control parameter. Under these conditions a system undergoing phase separation will reach an equilibrium state that minimizes its enthalpy $H_e = E + PV$.

However, as shown above, the Helmholtz free energy $F = E - TS$ seems to be the natural one to describe the decomposition process theoretically. What will be done here then is determine how the temperature and volume change in time during a pressure quench and subsequent decomposition. These time dependent values of T and V will then be inserted into the coefficients of the coarse-grained free energy \mathcal{F} to determine the evolution of the slow modes.

One difficulty with this scheme though is that the above construction of \mathcal{F} does not handle well changes in volume. With the coarse-grained cell size a fixed, the number of cells changes as the volume is changed. However, for a typical pressure change ΔP for the quenches in the binary liquids of interest, the fractional volume change $\frac{\Delta V}{V} \leq 10^{-5} \ll 1$. So, given the level of approximation of this theory, this ambiguity in the definition of the concentration field will be ignored.

Since both the temperature and volume will change if the pressure changes, two independent relations are needed to determine their time evolution. The first relation is as follows.

To move the near-critical binary liquid from the one-phase region toward the unstable portion of the two-phase region, the external pressure is dropped by a differential amount dP , increasing the system (average) volume by dV . No heat is allowed to flow between the system and the external world, so the average work done by the system on the external world (via a piston, say) equals the average change in the total system energy. Thus,

$$d\langle E_t \rangle = -PdV, \quad (\text{II.19})$$

where $d\langle E_t \rangle$ is given by Eq. (II.12) (though it is not zero in this case obviously).

What, though, is the pressure P ? In equilibrium,

$$P = P_r + P_{cg}, \quad (\text{II.20})$$

where $P_r = -(\frac{\partial F_r}{\partial V})_T$ and $P_{cg} = -(\frac{\partial F_{cg}}{\partial V})_T$ are the partial pressures of the reservoir and slow modes, respectively, with F_{cg} being defined below Eq.(II.18). However, spinodal decomposition is a non-equilibrium process. It necessarily does not allow the slow modes to relax completely during the quench. In the extreme case that the quench is so fast that the slow modes are frozen, the contribution of these modes to the pressure would be zero. Thus, the actual pressure of the liquid on the container walls should be less than that given by Eq.(II.20). On the other hand, it is assumed that the movement of the piston that causes the drop in external pressure is slow enough so that the degrees of freedom in the reservoir are able to remain in equilibrium. For example, any momentary density drop near the piston wall is rapidly distributed throughout the liquid so no turbulence or other inhomogeneous flow results.[28] Thus, $P \geq P_r$.

Estimates of P_{cg} , and the change of it, ΔP_{cg} , during the quench would be helpful here. As discussed above, upper bounds will be their equilibrium values. In equilibrium, P_{cg} is a finite function of ϵ and so will change little for a near-critical quench. So, an estimate of it at any point during the quench should be sufficient. Now, the number of slow modes is $N = \frac{V}{a^3} \sim \frac{V}{\xi_f^3}$, where ξ_f is the equilibrium correlation length at the final temperature T_f . Each slow mode will have an energy of order $k_B T_f \sim k_B T_c$, and so the equilibrium free energy of the slow modes is $F_{cg} \sim -\frac{V}{\xi_f^3} k_B T_c$. In equilibrium then,

$$P_{cg} \sim \frac{k_B T_c}{\xi_f^3}. \quad (\text{II.21})$$

The short wavelength concentration modes also contribute to \mathcal{F} , so Eq. (II.21) may be an underestimate, but it should be accurate within an order of magnitude. With $|\epsilon_f| \sim 10^{-5}$ for the quenches of 3MP+NE of BC [11], and using data from Table I, it is found that $P_{cg} \sim 1$ Pa in equilibrium. The experiments of BC were done near standard pressure at sea level, which is around 10^5 Pa. Thus,

$$\frac{P_{cg}}{P} \sim 10^{-5} \ll 1. \quad (\text{II.22})$$

Also, the absolute change in pressure during a typical quench for the BC experiments (e.g., $\epsilon_i = 10^{-5}$ to $\epsilon_f = -\epsilon_i$) was $|\Delta P| \simeq 10^4$ Pa. An upper bound on $|\Delta P_{cg}|$ is P_{cg} , so

$$\frac{|\Delta P_{cg}|}{|\Delta P|} \leq 10^{-4} \ll 1. \quad (\text{II.23})$$

Thus, $P \simeq P_r$ throughout the quench and decomposition process.

Eq.(II.19) is completed by obtaining expressions for dE_r and $d\langle\mathcal{E}[c]\rangle$. For this adiabatic case both the temperature and volume change, so

$$dE_r = \left(\frac{\partial E_r}{\partial T}\right)_V dT + \left(\frac{\partial E_r}{\partial V}\right)_T dV, \quad (\text{II.24})$$

Likewise, the change in the average coarse-grained energy is

$$d\langle\mathcal{E}[c]\rangle = \left\langle\frac{\partial\mathcal{E}[c]}{\partial V}\right\rangle dV + \frac{\partial\langle\mathcal{E}[c]\rangle}{\partial t} dt. \quad (\text{II.25})$$

It will be seen in the next section that $\left\langle\frac{\partial\langle\mathcal{E}[c]\rangle}{\partial V}\right\rangle \simeq \langle\mathcal{E}[c]\rangle/V$. As discussed above, the relative volume changes for the near-critical quenches with 3MP+NE were very small, so this term can be ignored. Combining eqs.(II.19), (II.24) and (II.25) gives a single equation relating dT and dV to dP (i.e., dP_r).

A second relation is that of the differential change in the reservoir pressure P_r to changes in temperature and volume:

$$dP_r = \left(\frac{\partial P_r}{\partial T}\right)_V dT + \left(\frac{\partial P_r}{\partial V}\right)_T dV. \quad (\text{II.26})$$

Combining Eqs. (II.19) and (II.24)-(II.26), and using standard thermodynamic relations [28, 29] gives

$$\frac{dT}{dt} = \left(\frac{\partial T}{\partial P_r}\right)_{S_r} \frac{dP}{dt} - \frac{1}{C_{Pr}} \frac{\partial\langle\mathcal{E}[c]\rangle}{\partial t}, \quad (\text{II.27})$$

and

$$\frac{dV}{dt} = -VK_{Sr} \frac{dP}{dt} - \frac{1}{T} \left(\frac{\partial T}{\partial P_r}\right)_{S_r} \frac{\partial\langle\mathcal{E}[c]\rangle}{\partial t}, \quad (\text{II.28})$$

where $\left(\frac{\partial T}{\partial P_r}\right)_{S_r} = \frac{VT\alpha_{pr}}{C_{Pr}}$. Here, $\alpha_{pr} = K_{Tr} \left(\frac{\partial P_r}{\partial T}\right)_V = \frac{1}{V} \left(\frac{\partial V}{\partial T}\right)_{P_r}$ is the reservoir isobaric thermal expansion coefficient, $C_{Pr} = C_{Vr} \frac{K_{Tr}}{K_{Sr}}$ is the reservoir isobaric heat capacity, $K_{Tr} = -\frac{1}{V} \left(\frac{\partial V}{\partial P_r}\right)_{T_r}$ is the reservoir isothermal compressibility, and $K_{Sr} = -\frac{1}{V} \left(\frac{\partial V}{\partial P_r}\right)_{S_r}$ is the reservoir adiabatic compressibility.

The meaning of the above equations is this: The pressure is changed at a known rate $\frac{dP}{dt}$ and work is done on the system. In the above approximation all the work is done on the reservoir ($\left(\frac{\partial T}{\partial P_r}\right)_{S_r}$ and K_{Sr} are reservoir functions). The reservoir reacts instantaneously and the temperature T and volume V change at rates given by the first terms in Eqs. (II.27) and II.28). The coupling between the work source and the slow modes is indirect. As the change in the reservoir causes T and V to change, the change in T and V causes the coefficients in $\mathcal{F}[c]$ to change. A change in $\mathcal{F}[c]$ causes the slow modes to be out of equilibrium. These modes then relax by exchanging energy with the reservoir at constrained pressure, causing T and V to change at a rate given by the second terms in Eqs. (II.27 and II.28).

Looking more closely, consider a quench from the one-phase to the two-phase region. For simplicity, assume that the quench is very fast so that all the slow modes will be frozen during it. Then during the quench $\frac{dT}{dt} \simeq \left(\frac{\partial T}{\partial P_r}\right)_{S_r} \frac{dP}{dt}$. The final temperature T_f is estimated (perhaps roughly) using the full system thermodynamic function $\left(\frac{\partial T}{\partial P}\right)_S$, where S is the total entropy.[14] Now, the total isobaric heat capacity, $C_P = C_V \frac{K_T}{K_S}$, where K_T and K_S are the total isothermal and adiabatic compressibility, respectively. Substituting this relation and that of C_{Pr} above into Eq.(II.17) gives:

$$C_{Pr} = \frac{K_{Tr}}{K_{Sr}} \frac{K_S}{K_T} C_P - \frac{K_{Tr}}{K_{Sr}} C_{Vcg}. \quad (\text{II.29})$$

However, since the contribution to P from the slow modes has been neglected, $K_S \simeq K_{Sr}$ and $K_T \simeq K_{Tr}$. Further, $K_T \simeq K_S$ at the temperatures of experimental interest. Thus,

$$C_{Pr} \simeq C_P - C_{cg}, \quad (\text{II.30})$$

where C_{cg} means either C_{Vcg} or C_{Pcg} . Further, from Tables I and II it can be seen that the singular part of the thermal expansion coefficient α_p is much smaller than the background part for the quenches we are considering. The slow modes contribute only (or almost only) to the singular part of α_p , which is much smaller than the background part for 3MP+NE; thus, $\alpha_{pr} \simeq \alpha_p$. So, since $\left(\frac{\partial T}{\partial P_r}\right)_{S_r} \simeq \frac{VT\alpha_p}{C_P - C_{cg}} > \frac{VT\alpha_p}{C_P} = \left(\frac{\partial T}{\partial P}\right)_S$, the temperature undershoots T_f and reaches a value T_{min} . Now after the quench the slow modes will relax and the temperature will change at a rate $\frac{dT}{dt} = -\frac{1}{C_P - C_{cg}} \frac{\partial\langle\mathcal{E}[c]\rangle}{\partial t}$. As the system phase separates $\frac{\partial\langle\mathcal{E}[c]\rangle}{\partial t} < 0$ and so the temperature will increase, reaching the equilibrium temperature T_f over time. On the other hand, since K_{Sr} and $\left(\frac{\partial T}{\partial P_r}\right)_{S_r}$ are both positive quantities, V increases monotonically to its final value V_f . As $t \rightarrow \infty$ the system reaches a state of minimum enthalpy.

To complete the theory, useful expressions for α_{pr} , C_{Pr} , \mathcal{F} and \mathcal{E} are needed. First, consider C_{Pr} which is given by Eq.(II.30). Since C_P is known, one could presumably determine C_{Pr} by calculating $C_{cg} \simeq C_{Vcg}$ using Eq.(II.18). However, a sufficiently accurate form of C_{cg} by this method possibly would require substantial calculation. Rather, C_{Pr} will be approximated by its average over the interval $\{\epsilon_i, \epsilon_f\}$, where ϵ_i is the initial value of ϵ . The justification for this approximation is that, as stated above, F_r is an analytic function of $T - T_c$, and so C_{Pr} is a non-singular function of ϵ . Then, presumably, C_{Pr} varies slowly around $\epsilon = 0$.

It will be shown in the next section that the only important temperature and volume (actually pressure) dependent parameter to appear in the decomposition theory will be ϵ . As such, the average coarse-grained energy

will also only be a function of ϵ . So,

$$C_{cg} \approx \frac{1}{T_c} \left(\frac{\partial \langle \mathcal{E}[c] \rangle}{\partial \epsilon} \right), \quad (\text{II.31})$$

and the partial derivative implies holding all parameters but ϵ fixed. With Eq.(II.31), averaging Eq. (II.30) over ϵ from the initial to the final temperatures, ϵ_i and ϵ_f , respectively, gives:

$$\begin{aligned} C_{Pr} &\approx \frac{1}{\Delta\epsilon} \int_{\epsilon_i}^{\epsilon_f} d\epsilon [C_P - C_{cg}] \\ &= \frac{1}{\Delta\epsilon} \left[\int_{\epsilon_i}^{\epsilon_f} d\epsilon C_P - \frac{1}{T_c} (\langle \mathcal{E}[c] \rangle_f - \langle \mathcal{E}[c] \rangle_i) \right], \end{aligned} \quad (\text{II.32})$$

where $\Delta\epsilon = \epsilon_f - \epsilon_i$. This approximation should be sufficient as long as $\epsilon_i \sim -\epsilon_f$, that is, the quenches are neither too deep nor too shallow.

To calculate the equilibrium function α_{pr} , consider a slow, differential change in the pressure P that allows the system to remain in equilibrium. Since this process is reversible, the entropy will remain constant. Under these conditions Eq.(II.27) can be written as

$$1 = \left\{ \frac{V\alpha_{pr}}{C_{Pr}} - \frac{1}{T_c} \frac{dT_c}{dP} \right\} \left(\frac{\partial P}{\partial \epsilon} \right)_S - \frac{1}{T_c C_{Pr}} \left(\frac{\partial \langle \mathcal{E}[c] \rangle}{\partial \epsilon} \right), \quad (\text{II.33})$$

where

$$\left(\frac{\partial P}{\partial \epsilon} \right)_S = T_c \left[\left(\frac{\partial T}{\partial P} \right)_S - \frac{dT_c}{dP} \right]^{-1}. \quad (\text{II.34})$$

is an equilibrium function that relates changes in pressure to changes in the scaled temperature at constant entropy. In terms of its components, $\left(\frac{\partial T}{\partial P} \right)_S = \frac{VT\alpha_p}{C_P}$. Combining Eqs. (II.30), (II.31), (II.33) and (II.34) give:

$$\alpha_{pr} = \alpha_p - \frac{dT_c}{dP} \frac{1}{VT_c} (C_P - C_{Pr}). \quad (\text{II.35})$$

Using Tables I and II it can be shown that the singular parts of α_p and C_P cancel in this equation. Thus, with the approximation above for C_{Pr} , α_{pr} is a constant.

With the above equations, it is now possible to compute the final temperature T_f for a quench knowing the initial temperature T_i and pressure change ΔP . Since decomposition is a non-equilibrium process, it is not expected that T_f will equal that computed using $\left(\frac{\partial T}{\partial P} \right)_S$, which assumes constant entropy.

As the experiments are near T_c it is useful to work with changes in ϵ rather than T . In terms of ϵ , Eq.(II.27) is:

$$\frac{C_{Pr}}{V} d\epsilon = \left(\alpha_{pr} - \frac{C_{Pr}}{VT_c} \frac{dT_c}{dP} \right) dP - \frac{1}{T_c V} d\langle \mathcal{E}[c] \rangle. \quad (\text{II.36})$$

Substituting Eq.(II.32) for C_{Pr} , Eq.(II.35) for α_{pr} , and then integrating from the initial to final state gives

$$\int_{\epsilon_i}^{\epsilon_f} d\epsilon \frac{C_P}{V} = \left(A_b - \frac{C_b}{VT_c} \frac{dT_c}{dP} \right) (P_f - P_i), \quad (\text{II.37})$$

where P_i and P_f are the initial and final pressures, respectively. Also, A_b and C_b are the background contributions to the total isobaric thermal expansion coefficient and isobaric heat capacity, respectively, which are the same above and below T_c (see Table I, but recognize that there the heat capacity is per unit mass).

Note that the average energy of the slow modes does not appear in Eq.(II.37). That is, $\langle \mathcal{E}[c] \rangle$ determines the time evolution, including the undershoot temperature T_{min} , but not the final temperature T_f . Also, Eq.(II.37) is the same equation that would be obtained by assuming a reversible, constant entropy process. In other words, the temperature rise produced during the phase separation exactly compensates for the temperature undershoot caused by the lack of equilibration of the slow modes during the quench.

It can be shown that this expression for the final temperature ϵ_f , Eq.(II.37), doesn't depend on the specific approximation, Eq.(II.32), for C_{Pr} . At the least, Eq.(II.37) will hold as long as C_{Pr} is given by Eq.(II.30) and the approximation for C_{cg} is consistent with the value of $\langle \mathcal{E}[c] \rangle$, which depends only on ϵ in equilibrium.

Rather, one reason for this constant entropy result is the use here of properties of a binary liquid in the critical region, which includes the neglect of the coarse-grained pressure P_{cg} in and out of equilibrium. If P_{cg} were not small, then the pressure response of the slow modes and thus the liquid would depend on the quench rate, so that if the quench were fast the fluid entropy would increase in a manner similar to that of a gas expanding into a vacuum. A second reason is that, while the entropy of the slow modes is not necessarily small (thus the reason for accounting for C_{cg}), the dominant proportion of its change during phase separation is already accounted for in an equilibrium, constant entropy, process to get to the final state. For example, the heat of unmixing is included in the equilibrium function $\left(\frac{\partial T}{\partial P} \right)_S$ in spite of that being one of constant entropy. Thus, the overall transfer of energy between degrees of freedom in this non-equilibrium process is not much different than if the process had been an equilibrium one, so whatever entropy increase that does occur is small enough so that it can safely be approximated as zero. Contrary to the original expectation then, the final temperature can be computed accurately by just integrating $\left(\frac{\partial T}{\partial P} \right)_S$.

B. Temperature Dependent Coarse-Grained Free Energy

The last elements of the adiabatic theory are expressions for the temperature dependent coarse-grained free energy and energy. In isothermal decomposition, \mathcal{F} is taken to have the usual Ginzburg-Landau form:

$$\mathcal{F}[u] = \int_{\Lambda} d\mathbf{r} \left[\frac{K}{2} (\nabla u(\mathbf{r}))^2 + f(u(\mathbf{r}) + c_0) \right], \quad (\text{II.38})$$

where $u(\mathbf{r}) \equiv c(\mathbf{r}) - c_0$ is the deviation of the local concentration from its average c_0 . Also, $f(c)$ is the free energy density of a uniform system at concentration c , and the gradient term is the lowest order correction to the free energy from deviations of $u(\mathbf{r})$ from zero.[30] In LBM and KO, the implicit cut-off is set to be inversely proportional to the correlation length at the quenched temperature, T_f , i.e., $\Lambda \sim 1/\xi_f$. Further, these theories also choose $f(c)$ to have the standard “ φ^4 ” form, it being the dominant correction to the quadratic term in the critical region.[25]

Given this, follow LBM and let

$$f(c) = \frac{k_B T_f f_1}{\xi_f^3} \phi(x), \quad (\text{II.39})$$

where

$$\phi(x) = \frac{\zeta}{2} x^2 + \frac{\lambda_4}{4} x^4. \quad (\text{II.40})$$

Here, ζ and λ_4 are constants to be determined. Also, $x = \frac{c-c_c}{u_{sf}}$ is a reduced concentration, with $u_{sf} = B|\epsilon_f|^\beta$ being half the miscibility gap at the quenched temperature T_f , so that the scaled free energy density $\phi(x)$ is symmetric about the critical concentration. Last, $f_1 = \frac{\xi_f^3 u_{sf}^2}{\chi_f}$, where ξ_f and χ_f are the correlation length and susceptibility, respectively, at T_f . In the critical region hyperscaling holds,[29] so $f_1 = \frac{(\xi_0^-)^3 B^2}{\Gamma^-}$, which is a temperature independent, dimensionless ratio of two-phase amplitudes.

Last, the gradient energy coefficient

$$K = \lambda_K \frac{k_B T_f \xi_f^2}{\chi_f}, \quad (\text{II.41})$$

where $\chi_f = \Gamma^- |\epsilon_f|^{-\gamma}$ is the susceptibility at T_f , and λ_K is a dimensionless number very close to unity.

How then should \mathcal{F} be generalized to describe kinetics in which the temperature is not constant? While the early-stage theories of KO and LBM can be used for computing equilibrium states, they are not intended to describe properly static critical phenomena. In spite of this, they do incorporate fluctuations to some degree. Thus, it can be expected that these fluctuations will at least shift the apparent distance from the critical point, in a manner similar to how they shift the coexistence concentrations away from the minima of $f(c)$. So a correction for this shift in T_c must be made in \mathcal{F} .

What will be done here is just assume a simple temperature dependent form for \mathcal{F} and compute its coefficients. Then, the free energy will be examined to determine how well it predicts some equilibrium properties of a critical binary mixture such as the equation of state and susceptibility. If the free energy gives satisfactory results in regions important to the adiabatic decomposition theory, then its form and the scheme used to compute it will be considered adequate.

In that spirit, and given the arguments above (including those leading to Eq.(II.10)), assume that the dominant temperature dependence in the theory is in ζ and let that parameter be linear in ϵ :

$$\zeta \rightarrow \zeta(\epsilon) \approx (\lambda_2 - \lambda_0) \frac{\epsilon}{|\epsilon_f|} - \lambda_0. \quad (\text{II.42})$$

So, $\zeta(0) = -\lambda_0$ and $\zeta(\epsilon_f) = -\lambda_2$, assuming $\epsilon_f < 0$.

Since the experiments are in the critical region, any other temperature or volume dependence of \mathcal{F} will be ignored. As T_c itself changes if the density changes, ϵ will be a function of both T and V . However, for a system at constrained pressure, T_c is a function of pressure only, so ϵ will be considered a function of T and P rather than T and V . In that manner, the equation of motion for V , Eq.(II.28), will not be used.

With Eqs. (II.10) and (II.38)-(II.42), the average coarse-grained free energy

$$\langle \mathcal{E}[c] \rangle \simeq -(\lambda_2 - \lambda_0) \frac{1}{2|\epsilon_f|} \frac{k_B T_f f_1 V}{\xi_f^3} \langle x^2 \rangle. \quad (\text{II.43})$$

The one-point average $\langle x^2 \rangle$ can be obtained from the structure factor or one-point probability density, these quantities being the subject of the next section. The computation of the λ_i parameters will be described in Sec. V below.

III. HYDRODYNAMIC THEORY

In this section, the hydrodynamic KO theory of early-stage decomposition is described briefly. It is considered to be the most successful numerical theory of decomposition in critical binary fluids. It, like LBM, is built upon the Master equation vein of the theory of stochastic processes.[31] The KO theory consists of a set of equations that describe the time evolution of the structure factor $\hat{S}(k, t)$. Contact with experiment is made by relating $\hat{S}(k, t)$ to the scattered radiation intensity $I(k, t)$. [32]

Now, let $u_{\mathbf{k}}$ be the Fourier transform of the concentration deviation $u(\mathbf{r})$. The structure factor $\hat{S}(k)$ is defined as

$$\hat{S}(k) = \langle |u_{\mathbf{k}}|^2 \rangle, \quad (\text{III.1})$$

and is the Fourier transform of the concentration-concentration correlation function

$$S(\mathbf{r} - \mathbf{r}_0) = \langle u(\mathbf{r}) u(\mathbf{r}_0) \rangle. \quad (\text{III.2})$$

This function can be obtained from theory by taking moments of $\rho([u], t)$, which, as mentioned above, is the probability density that the system is in a coarse-grained configuration $[u]$ at time t .

In KO theory, the time evolution of the probability density $\rho([u], t)$ is determined by a Fokker-Planck equation [10]:

$$\frac{\partial \rho}{\partial t} = [\mathcal{L}_1 + \mathcal{L}_2] \rho, \quad (\text{III.3})$$

where the operators are given by

$$\mathcal{L}_1 = - \int d\mathbf{r}_1 d\mathbf{r}_2 \frac{\delta}{\delta u(\mathbf{r}_1)} \nabla_1^2 L_\Lambda(\mathbf{r}_1 - \mathbf{r}_2) \left[\frac{\delta \mathcal{F}}{\delta u(\mathbf{r}_2)} + k_B T \frac{\delta}{\delta u(\mathbf{r}_2)} \right], \quad (\text{III.4})$$

and

$$\mathcal{L}_2 = \int d\mathbf{r}_1 d\mathbf{r}_2 \frac{\delta}{\delta u(\mathbf{r}_1)} \nabla_1 u(\mathbf{r}_1) \cdot \mathbf{T}(\mathbf{r}_1 - \mathbf{r}_2) \cdot \nabla_2 u(\mathbf{r}_2) \left[\frac{\delta \mathcal{F}}{\delta u(\mathbf{r}_2)} + k_B T \frac{\delta}{\delta u(\mathbf{r}_2)} \right]. \quad (\text{III.5})$$

Here, $\frac{\delta}{\delta u(\mathbf{r})}$ is a functional derivative with respect to the concentration field at the point \mathbf{r} , and $\mathbf{T}(\mathbf{r})$ is the Oseen tensor with components $T_{\alpha\beta} = \frac{1}{8\pi\eta_s r} [\delta_{\alpha\beta} + \hat{r}_\alpha \hat{r}_\beta]$, with η_s being the hydrodynamic shear viscosity and $\hat{r} \equiv \mathbf{r}/r$.

Eqs. (III.3-III.5) describe phase separation driven by overdamped fluid flow, the flow in turn caused by gradients in the local chemical potential, $\mu(\mathbf{r}) = \frac{\delta \mathcal{F}[u]}{\delta u(\mathbf{r})}$. These equations are renormalized versions[33] of bare stochastic equations[34], which are formally equivalent to the Langevin equations of Model H of critical dynamics[35] in the overdamped approximation.

The operator \mathcal{L}_1 results from integrating out concentration fluctuations of wavenumber $k > \Lambda$. The Onsager function $L_\Lambda(r)$ that appears in \mathcal{L}_1 is weakly non-local and couples these short-wavelength concentration modes, *via* the fluid velocity field, to the long-wavelength modes $k < \Lambda$. $L_\Lambda(r)$ is the inverse Fourier transform of [33]:

$$\hat{L}_\Lambda(k_1) = \frac{1}{k_1^2} \int \frac{d\mathbf{k}_2}{(2\pi)^3} \mathbf{k}_1 \cdot \hat{\mathbf{T}}(\mathbf{k}_1 - \mathbf{k}_2) \cdot \mathbf{k}_1 \hat{S}_{eq}(k_2). \quad (\text{III.6})$$

Here, the integral over k_2 runs from Λ to an upper cut-off which is approximated as ∞ . $\hat{\mathbf{T}}(\mathbf{k})$ is the Fourier transform of the Oseen tensor with components $\frac{1}{\eta_s k^2} (\delta_{\alpha\beta} - \hat{k}_\alpha \hat{k}_\beta)$. $\hat{S}_{eq}(k)$ is the equilibrium structure factor of mode k ($> \Lambda$), and is taken to have a Lorentzian form:

$$\hat{S}_{eq}(k) = \frac{\chi}{1 + (k\xi)^2}, \quad (\text{III.7})$$

where χ and ξ are the susceptibility and correlation length, respectively, at temperature ϵ and concentration c_0 . Clearly, as the temperature changes, $\hat{S}_{eq}(k)$, and therefore $\hat{L}_\Lambda(k)$, will be changing also. However, it can be shown [33] that a reasonable approximation to Eq. (III.6) is

$$\hat{L}_\Lambda \simeq \frac{\chi}{3\pi^2 \xi^2 \eta_s \Lambda}. \quad (\text{III.8})$$

Making use of Tables I and II for χ, ξ and η_s , it is found that \hat{L}_Λ has a weak temperature dependence. Thus, if the quenches are relatively fast, $\hat{S}_{eq}(k)$ can be set to its value at the final equilibrium temperature ϵ_f . Further, the weak temperature dependence of the viscosity η_s will also be ignored. Then with these approximations, the only temperature dependence in (III.3) appears in the coarse-grained free energy, $\mathcal{F}[u]$.

An equation of motion for the structure factor $\hat{S}(k, t)$ was derived by KO using Eqs. (II.38) and (III.3-III.6). To evaluate two-point correlation functions in \mathcal{L}_1 other than $S(r)$, they used the LBM ansatz for the two-point probability density:

$$\rho_2^{lbm}(u_1, u_2) = \rho_1(u_1)\rho_1(u_2) \left[1 + \frac{u_1 u_2}{\langle u^2 \rangle^2} S(r_{12}) \right], \quad (\text{III.9})$$

where $r_{12} \equiv |\mathbf{r}_1 - \mathbf{r}_2|$, $u_1 \equiv u(\mathbf{r}_1)$, etc. This self-consistent linear approximation is expected to work best during the early stage of decomposition when the growing domains are not much larger than a few equilibrium correlation lengths and sharp interfaces have not yet formed.[6] Implicit in the LBM derivation is a constraint that averages taken with respect to ρ_2 must reduce to their exact form in the limit $r_{12} \rightarrow 0$. That is, for arbitrary functions $h(u)$ and $g(u)$, $\langle h(u_1)g(u_2) \rangle \rightarrow \langle h(u)g(u) \rangle$ as $r_{12} \rightarrow 0$, where the latter average is taken with respect to the one-point probability density $\rho_1(u)$. Implementing this constraint in a simple way, and using the ansatz above, gives an equation for ρ_2 :

$$\rho_2(u_1, u_2) \approx \rho_2^{lbm}(u_1, u_2) + a^3 \delta(\mathbf{r}_1 - \mathbf{r}_2) \left[\rho_1(u_1)\delta(u_1 - u_2) - \rho_2^{lbm}(u_1, u_2) \Big|_{r_{12} \rightarrow 0} \right]. \quad (\text{III.10})$$

The \mathcal{L}_2 contribution to $\hat{S}(k, t)$ contains a four-point correlation function. KO argued that during the early stage of decomposition the coupling between modes in this correlation function would be close to gaussian. In this approximation the four-point correlation function reduces to a product of two-point ones.[10]

The result is:

$$\begin{aligned} \frac{\partial \hat{S}(k_1)}{\partial t} = & -2\hat{L}_\Lambda(k_1)k_1^2 \left[(Kk_1^2 + A)\hat{S}(k_1) - k_B T \right] \\ & + 2 \int^\Lambda \frac{d\mathbf{k}_2}{(2\pi)^3} \mathbf{k}_1 \cdot \hat{\mathbf{T}}(\mathbf{k}_1 - \mathbf{k}_2) \cdot \mathbf{k}_1 \left[K(k_2^2 - k_1^2)\hat{S}(k_2)\hat{S}(k_1) + k_B T \hat{S}(k_2) - k_B T \hat{S}(k_1) \right]. \end{aligned} \quad (\text{III.11})$$

Here,

$$A = \frac{1}{\langle u^2 \rangle} \langle u \frac{\partial f(u + c_0)}{\partial u} \rangle, \quad (\text{III.12})$$

where the averages are taken with respect to $\rho_1(u)$.

It can be shown[10] that the operator \mathcal{L}_2 doesn't contribute directly to the equation of motion for $\rho_1(u)$. Given this, the derivation of the equation of motion for $\rho_1(u, t)$ from Eq.(III.3) is almost identical to the one in LBM. It is found:

$$\frac{\partial \rho_1(u)}{\partial t} = \frac{\partial}{\partial u} \left[G(u) \rho_1(u) + k_B T \frac{L}{a^3} \frac{\partial \rho_1(u)}{\partial u} \right], \quad (\text{III.13})$$

where

$$G(u) = W \frac{u}{\langle u^2 \rangle} + L \left[\frac{\partial f}{\partial u} - \langle \frac{\partial f}{\partial u} \rangle - \frac{u}{\langle u^2 \rangle} \langle u \frac{\partial f}{\partial u} \rangle \right], \quad (\text{III.14})$$

$$W = \int_0^\Lambda \frac{dk}{2\pi^2} k^4 \hat{L}_\Lambda(k) (Kk^2 + A) \hat{S}(k), \quad (\text{III.15})$$

and

$$L = a^3 \int_0^\Lambda \frac{dk}{2\pi^2} k^4 \hat{L}_\Lambda(k). \quad (\text{III.16})$$

For the initial conditions of these equations, the equilibrium solution of them will be used. Since the equilibrium form should be independent of the mechanism of equilibration, to simplify the result, the term $\nabla_1^2 L_\Lambda(\mathbf{r}_1 - \mathbf{r}_2)$ can be replaced with $\delta(\mathbf{r}_1 - \mathbf{r}_2)$ in Eq.(III.4) above. With this, and setting the RHS of Eq.(III.13) to zero yields

$$\rho_{1eq}(u) = \exp \left[-\frac{a^3}{k_B T} (f(u + c_0) - u \langle \frac{\partial f}{\partial u} \rangle) - \frac{a^3 K}{2k_B T} \frac{u^2}{\langle u^2 \rangle} \int_0^\Lambda \frac{dk}{2\pi^2} k^4 \hat{S}_{eq}(k) + b_0 \right] \quad (\text{III.17})$$

where b_0 is a normalization constant. The equilibrium structure factor is obtained by setting the RHS of

Eq.(III.11) to zero, giving

$$\hat{S}_{eq}(k) = \frac{k_B T}{Kk^2 + A}, \quad (\text{III.18})$$

with A being given by Eq.(III.12) above, but now computed using Eq.(III.17).

These kinetic and equilibrium equations were solved numerically.

IV. SCALING AND NUMERICAL SOLUTION

A. Scaling of the Equations

For numerical computation, it is helpful to scale the above equations. While in adiabatic decomposition the temperature will necessarily be changing with time after the quench, the final equilibrium temperature will still be the relevant one. So, as in KO and LBM, the scaling will be done with respect to system properties at ϵ_f .

Define the scaled wavevector cut-off $\alpha^* = \Lambda \xi_f$, where α^* is a number close to 1. Define also the dimensionless wavevector, $q = k \xi_f$; distance, $\tilde{r} = r / \xi_f$; structure factor, $\tilde{S}(q) = \hat{S}(k) / \chi_f$; relative concentration, $y = u / u_{sf}$; average concentration, $x_0 = \frac{c_0 - c_c}{u_{sf}}$; and time, $\tau = \frac{k_B T}{6\pi\eta_s \xi_f^3} t$.

As for LBM, the cell volume $a^3 = \left(\int \frac{d\mathbf{k}}{(2\pi)^3} \right)^{-1} = \frac{6\pi^2}{(\alpha^*)^3} \xi_f^3$.

It is convenient to scale the Onsager function, Eq.(III.6), as

$$\begin{aligned} \sigma(q) &= \frac{6\pi\xi_f\eta_s}{\chi_f} \hat{L}_\Lambda(q/\xi_f) \\ &= K(q) - \frac{3}{2\pi} \int_0^{\alpha^*} dm Q(q/m) \frac{1}{1+m^2} \end{aligned} \quad (\text{IV.1})$$

where $K(q)$ is a Kawasaki function[10]:

$$K(q) = \frac{3}{4} \left[\left(\frac{1}{q} - \frac{1}{q^3} \right) \arctan(q) + \frac{1}{q^2} \right], \quad (\text{IV.2})$$

and

$$Q(x) = \frac{1}{2} \left[\frac{1}{x} + \frac{1}{x^3} \right] \ln \left| \frac{1+x}{1-x} \right| - \frac{1}{x^2}. \quad (\text{IV.3})$$

Changing to the new scaled variables and performing any angular integration, the equation of motion for the structure factor becomes:

$$\begin{aligned} \frac{\partial \tilde{S}(q)}{\partial \tau} &= -2\sigma(q)q^2 \left[(\lambda_K q^2 + \tilde{A}) \tilde{S}(q) - 1 \right] \\ &\quad + \frac{3}{\pi} q^2 \int_0^{\alpha^*} dm Q(q/m) \left[\lambda_K (m^2 - q^2) \tilde{S}(q) \tilde{S}(m) + \tilde{S}(m) - \tilde{S}(q) \right], \end{aligned} \quad (\text{IV.4})$$

where

$$\tilde{A} = \frac{1}{\langle y^2 \rangle} \langle y \frac{\partial \phi(y + x_0)}{\partial y} \rangle. \quad (\text{IV.5})$$

The kinetic equation for the one-point probability den-

sity ρ_1 is now

$$\frac{\partial \rho_1(y)}{\partial \tau} = \omega \frac{\partial}{\partial y} \left[g(y) \rho_1(y) + \frac{\partial \rho_1(y)}{\partial y} \right], \quad (\text{IV.6})$$

where

$$\omega = \frac{1}{f_1} \int_0^{\alpha^*} \frac{dq}{2\pi^2} q^4 \sigma(q), \quad (\text{IV.7})$$

and

$$g(y) = \frac{\tilde{W}y}{\langle y^2 \rangle} + f_0 \left(\frac{\partial \phi}{\partial y} - \langle \frac{\partial \phi}{\partial y} \rangle - y \tilde{A} \right), \quad (\text{IV.8})$$

with

$$\tilde{W} = \frac{1}{f_1 \omega} \int_0^{\alpha^*} \frac{dq}{2\pi^2} q^4 \sigma(q) (\lambda_K q^2 + \tilde{A}) \tilde{S}(q). \quad (\text{IV.9})$$

Here, $f_0 = 6\pi^2 f_1 / (\alpha^*)^3$.

Last, using Eq.(II.27), it can be found that the equation of motion for the reduced temperature is:

$$\frac{d\epsilon}{d\tau} = \left[\frac{\alpha_{Pr}}{\rho_c C_{Pr}} - \frac{1}{T_c} \frac{dT_c}{dP} \right] \frac{dP}{d\tau} - \frac{k_B}{\xi_f^3 \rho_c C_{Pr}} \frac{d\tilde{\epsilon}}{d\tau}, \quad (\text{IV.10})$$

where ρ_c is the critical mass density and C_{Pr} is now the reservoir heat capacity per unit mass, and the average coarse-grained energy, Eq. (II.43), properly scaled, is:

$$\begin{aligned} \tilde{\epsilon} &= \frac{\xi_f^3}{V k_B T_f} \langle \mathcal{E}[c] \rangle \\ &= -(\lambda_2 - \lambda_0) \frac{f_1}{2|\epsilon_f|} \langle x^2 \rangle. \end{aligned} \quad (\text{IV.11})$$

The scaled form of the equilibrium equations, (III.17) and (III.18), are, respectively,

$$\begin{aligned} \rho_{1eq}(y) &= \exp \left[-f_0 \left(\phi(y + x_0) - y \langle \frac{\partial \phi}{\partial y} \rangle \right) \right. \\ &\quad \left. - \frac{y^2}{\langle y^2 \rangle} \frac{f_0 \lambda_K}{2f_1} \int_0^{\alpha^*} \frac{dq}{2\pi^2} q^4 \tilde{S}_{eq}(q) + b_0 \right], \end{aligned} \quad (\text{IV.12})$$

and

$$\tilde{S}_{eq}(q) = \frac{1}{\lambda_K q^2 + \tilde{A}}, \quad (\text{IV.13})$$

where again b_0 is a normalization constant.

From these equations it can be seen that an (linear) isothermal quench and subsequent decomposition is completely specified by the quench time τ_{quench} , the ratio of the initial to the final scaled temperature, $\frac{\epsilon_i}{\epsilon_f}$, and the average concentration x_0 . In addition to the properties of the particular fluid one wants to study, an adiabatic quench is completely specified by these same quantities plus the change in pressure, ΔP . The predictions of the theory are also somewhat dependent on the value of the scaled cut-off α^* . However, the degree of this dependence will be minimized by the method of computing the λ_i parameters in the coarse-grained free energy, discussed below.

B. Numerical Solution

The scaled adiabatic equations were solved numerically as follows.

$\tilde{S}(q)$ was solved on a grid of N_q points $q_i = i\Delta q$, $i = 1, \dots, N_q$ in q -space, with spacing $\Delta q = 2\alpha^*/N_q$. $\tilde{S}(q)$ was set to zero for all grid points $q_i > \alpha^*$. The reason the grid was extended in this manner was to be able to inverse Fourier transform $\tilde{S}(q)$ if need be. The q grid point number N_q was set to $2^9 = 512$ for any run with a maximum time $\tau_{max} \leq 10^3$, and was set to $2^{10} = 1024$ for longer runs of $10^3 < \tau_{max} \leq 10^4$. Similarly, $\rho_1(y)$ was solved on a grid of N_y equally spaced points y_i , $i = 1, \dots, N_y$ in y -space, with $y_1 = y_{min} + \Delta y/2$, $y_2 = y_{min} + 3/2\Delta y$, and $y_{N_y} = y_{max} - \Delta y/2$, where $\Delta y = N_y/(y_{max} - y_{min})$ and $y_{min} = -y_{max}$. To ensure that $\rho_1(y)$ could model properly behavior near the coexistence curve at ϵ_f , y_{max} was set to 2.5. Also, $N_y = 120$ for all results shown in this work. It was found that no result shown here changed appreciably if N_q and N_y were increased beyond the above values.

Now, the adiabatic theory consists of ODE's for $\tilde{S}(q, \tau)$ and $\epsilon(\tau)$, and a PDE for $\rho_1(y, \tau)$. To simplify the computation, the PDE for $\rho_1(y, \tau)$ was converted into a set of coupled ODE's, using a simple finite difference scheme. Let ρ_{1i} and g_i be the values of $\rho_1(y)$ and $g(y)$ at the i th grid point y_i . Then, Eq. (IV.6) becomes

$$\begin{aligned} \frac{d\rho_{1i}}{d\tau} &= \omega \left[g_{i+1} \rho_{1(i+1)} - g_{i-1} \rho_{1(i-1)} \right] / (2\Delta y) \\ &\quad + \omega \left[\rho_{1(i+1)} + \rho_{1(i-1)} - 2\rho_{1i} \right] / \Delta y^2, \end{aligned} \quad (\text{IV.14})$$

with the boundary conditions $\rho_{11} = \rho_{1N_y} = 0$. A total of $N = N_q/2 + N_y - 2 + 1$ ODE's result. The integration of these in time was done using the Bulirsch-Stoer method.[36] The structure factor equations are stiff in the sense that the relaxation of the high- q modes is much faster than the low- q ones. The Bulirsch-Stoer method is not usually used for solving such an ODE type. Given that, initially the equations were also solved using a commercial package built for solving stiff ODE's.[37] It was found that both methods yielded the same results.

In past work, the PDE for $\rho_1(y)$ was solved instead using the much faster "double gaussian" method.[6] This method was analyzed for on-critical quenches, $x_0 = 0$, and found to give essentially identical results to the finite difference method at early times. However, it overestimated the phase separation at later times when the wavevector q_m of the peak of the structure factor was less than 0.3. For the BC experiments, data was available out to times such that $q_m < 0.2$. As a consequence, this approximation was not used here.

For each timestep, ρ_1 was normalized to prevent accumulation of round-off errors. The first moment, $\langle y \rangle$ of ρ_1 was monitored to ensure that it remained zero. The second moment of ρ_1 and the integral of $\tilde{S}(q)$ were also monitored to ensure they both gave the same result for $\langle y^2 \rangle$.

The equilibrium equations, (IV.12) and (IV.13), were solved using the same grids for q and y , though here N_q was set to $2^{12} = 4096$. Simple iteration was used for them. The initial guess for $\tilde{S}_{eq}(q)$ was a scaled version of Eq.(III.7) at the relevant initial ϵ and x_0 . However, if the LBM solution of $\tilde{S}_{eq}(q)$ differed appreciably from the known value, bootstrap, i.e., a previous guess at a nearby temperature and concentration, was used instead.

V. COMPUTING THE COARSE-GRAINED FREE ENERGY

The last ingredients of the theory are values for the λ_i parameters in the coarse-grained free energy, defined in Sec. II B above. Similar to LBM, these parameters were determined by using \mathcal{F} to compute the equilibrium structure factor and chemical potential on coexistence at the final temperature ϵ_f , and at the critical point $\epsilon = 0$. There are a number of ways to accomplish this task. The one probably most accurate for the least amount of effort is to use the LBM equilibrium solution for $\tilde{S}(q)$ and $\rho_1(y)$. [38] This scheme was used here. It amounts to applying N equilibrium conditions to the LBM equations for the N unknowns, and finding the solution of them using the Newton-Raphson method. [36] Here, all derivatives required by this method were computed numerically.

For here and elsewhere in this work, the free energy amplitude f_1 was set to 0.210, consistent with the critical amplitude values in Table II.

On coexistence, $\epsilon = \epsilon_f$ and $x_0 = 1$, the scaled equilibrium structure factor $\tilde{S}(q) = 1/(1 + q^2)$. Two relations obtained from this equation were $\tilde{S}(0) = 1$ and

$$\begin{aligned} \langle y^2 \rangle &= \frac{1}{2\pi^2 f_1} \int_0^{\alpha^*} dq q^2 \tilde{S}(q) \\ &= \frac{1}{2\pi^2 f_1} [\alpha^* - \arctan(\alpha^*)]. \end{aligned} \quad (\text{V.1})$$

A third relation is that the exchange chemical potential must vanish on coexistence: $\tilde{\mu} = \langle \frac{\partial \phi}{\partial x} \rangle = 0$. These three equations are sufficient to determine λ_K , λ_2 and λ_4 for any cut-off α^* . The last parameter λ_0 was determined by requiring that $\tilde{S}(0) = \infty$, i.e., $\tilde{A} = 0$, at the critical point, $\epsilon = 0$ and $x_0 = 0$. Values for these λ_i 's for various cut-offs are shown in Table III below. Note that the value of λ_0 does not depend on the *form* of the temperature dependence of ζ , Eq.(II.42), only that it reduce to $-\lambda_0$ at $\epsilon = 0$.

To justify some approximations made previously, it is helpful to examine the predictions of the equilibrium LBM theory on-critical above T_c and on-coexistence below it.

Figure 1 shows LBM predictions for the equilibrium, on-critical inverse susceptibility $\tilde{S}^{-1}(0)$ as a function of $\frac{\epsilon}{|\epsilon_f|} > 0$ for two cutoff values $\alpha^* = 1$ and $\pi/2$. Also shown are the expected scaling predictions for a simple binary

fluid (3-D Ising universality class): $\tilde{S}(0)^{-1} = \Gamma^- / \Gamma^+ |\frac{\epsilon}{\epsilon_f}|^\gamma$ where the amplitude ratio and exponent are obtained from Table II. For $\frac{\epsilon}{|\epsilon_f|} \ll 1$, it is found that LBM also predicts scaling behavior, with the exponent γ approximately equal to the mean spherical model value of 2. [29] Since the accepted 3-D Ising value of $\gamma \approx 1.240$, the LBM theory does not perform well in this limit as expected. However, it can seen for higher temperatures the theory performs much better. For $0.5 \leq \frac{\epsilon}{|\epsilon_f|} \leq 10$, the LBM predictions for $\tilde{S}(0)$ are within 10% and 20% of the exact values for $\alpha^* = 1$ and $\alpha^* = \pi/2$, respectively. For higher temperatures, the agreement lessens, but $\tilde{S}(0)$ is small there anyways. It was found that the predictions of the hydrodynamic theory are pretty much insensitive to such small variations in the initial conditions. (More important is that $\tilde{S}(q)$ and $\rho_1(y)$ be consistent with each other.)

Define an effective susceptibility exponent

$$\gamma_{eff} = -\ln[\tilde{S}(0, \epsilon_1)/\tilde{S}(0, \epsilon_2)] / \ln[\epsilon_1/\epsilon_2], \quad (\text{V.2})$$

where the temperatures ϵ_1 and ϵ_2 are close to each other in some sense. Then, over this temperature range, $0.5 \leq \frac{\epsilon}{|\epsilon_f|} \leq 10$, LBM predicts that γ_{eff} varies from 1.39 down to 1.10 for $\alpha^* = 1$, and 1.47 down to 1.15 for $\alpha^* = \pi/2$. Also, for $\alpha^* = 1$ and $\frac{\epsilon}{|\epsilon_f|} = 1.5$, and $\alpha^* = \pi/2$ and $\frac{\epsilon}{|\epsilon_f|} = 2.3$, $\gamma_{eff} = 1.24$, i.e., is exact.

Thus, the LBM theory seems to describe properly the temperature dependence of critical fluctuations within a window near $\frac{\epsilon}{|\epsilon_f|} = 1$. It is concluded then that using the equilibrium LBM theory, along with \mathcal{F} defined in Sec. II B above, to give initial conditions for $\tilde{S}(q)$ and $\rho_1(y)$ is acceptable as long as the quenches are not too deep, $\frac{\epsilon_i}{|\epsilon_f|} > 0.5$.

Examining the LBM predictions for the two-phase coexistence curve $\epsilon(x_0)$ is also illuminating. Figure 2 shows $\epsilon(x_0)$ for positive x_0 (the curve is symmetrical about $x_0 = 0$) for cutoffs $\alpha^* = 1$ and $\pi/2$. Also shown is the accepted scaling form for a system in the 3-D Ising universality class: $\epsilon(x_0) \sim -|x_0|^{1/\beta}$, with $\beta \approx 0.33$. Thus, $\epsilon(x_0)$ should have a maximum at $x_0 = 0$. However, as can be seen, instead of a maximum at $x_0 = 0$, the LBM predictions overshoot $\epsilon = 0$ and have a maximum at around $x_0 = 0.2$ and 0.25 for $\alpha^* = 1$ and $\pi/2$, respectively. [39] Thus, the LBM theory should not be used to describe the initial state for quenches that are deep, $\frac{\epsilon}{|\epsilon_f|} \ll 1$, and off-critical. Also, contrary to its behavior above T_c , the LBM predictions for γ_{eff} below T_c are always below the

TABLE III. Coarse-grained free energy coefficients λ_i for various wavevector cut-offs α^* .

α^*	λ_K	λ_0	λ_2	λ_4
1.0	1.0	0.3203	0.6915	0.6020
1.4	1.0	0.5169	0.8734	0.6704
$\pi/2$	1.0	0.6054	0.9533	0.6913

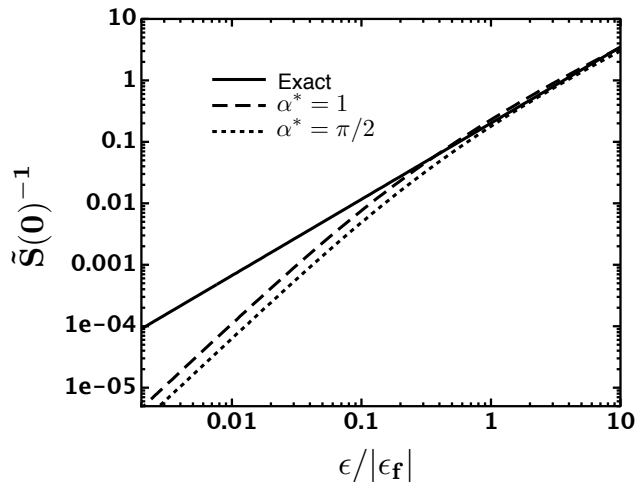


FIG. 1. LBM predictions, using the temperature dependent coarse-grained free energy defined in Sec. II B, for the equilibrium, one-phase, on-critical, inverse susceptibility $\tilde{S}(0)^{-1}$ as a function of the scaled temperature $\frac{\epsilon}{|\epsilon_f|} > 0$. Results for two cut-offs α^* are shown, along with “exact” scaling values.

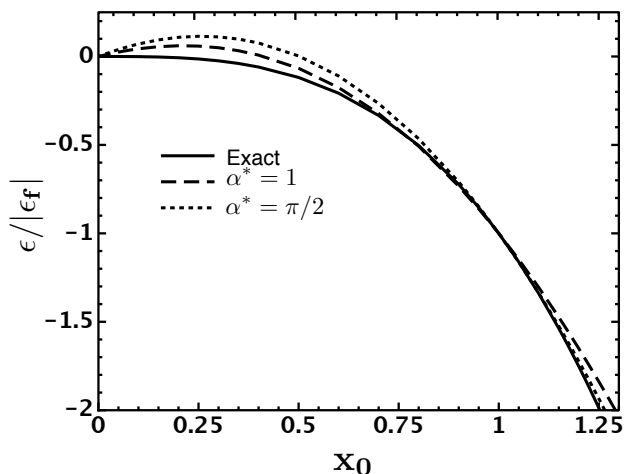


FIG. 2. LBM predictions, using the temperature dependent coarse-grained free energy defined in Sec. II B, for the coexistence curve $\epsilon(x_0)$ for two cut-offs $\alpha^* = 1$ and $\pi/2$. Also shown is the “exact” scaling form in the critical region, $\frac{\epsilon}{|\epsilon_f|} = -x_0^{1/\beta}$, where $\beta \approx 0.33$.

accepted 3-D Ising scaling value of 1.240, at best reaching 0.9 at $\frac{\epsilon}{|\epsilon_f|} = -2.0$.

On the other hand, the theory’s predictions for an effective β exponent, β_{eff} , defined analogously to γ_{eff} in Eq. (V.2) above, are near the accepted 3-D Ising value for temperatures near ϵ_f . For $\alpha^* = 1$ and $\frac{\epsilon}{|\epsilon_f|} = -0.85$, and $\alpha^* = \pi/2$ and $\frac{\epsilon}{|\epsilon_f|} = -1$, β_{eff} equals the accepted β value of 0.328. Also, for temperatures near ϵ_f , the predictions of LBM for $\epsilon(x_0)$ are in good agreement with the accepted values in the range $-2.0 \leq \frac{\epsilon}{|\epsilon_f|} \leq -0.5$.

As will be seen below, the adiabatic theory predicts that the temperature undershoot after an on-critical quench of 3MP+NE does not go below $-2\epsilon_f$. Thus, if the quenches are fast, the on-coexistence equilibrium predictions of the LBM theory should be acceptable.

It is concluded that if the quenches are not too deep, and are fast enough so that the fluid spends little time exploring the region near T_c , then the temperature dependent coarse-grained free energy defined in Sec. II B is adequate.

VI. RESULTS

In this section, general predictions of the adiabatic and isothermal decomposition theories are discussed, and then the theories are compared with experiment. In an unpublished work, Schwartz showed that the original numerical scheme of KO was not quite right,[40] leading to erroneous results for the structure factor at intermediate and late times. Given this, aspects of the isothermal KO theory by itself will also be discussed.

A. General Predictions

In the isothermal decomposition theory, the equations scale completely. That is, no system or temperature dependent parameter appears in the theory when the equations are scaled using parameters appropriate to the critical region. Thus, if initial (and quench) conditions are ignored, the theory predicts that if the experimental data is appropriately rescaled then the data should superimpose for any binary fluid and any quench temperature.

However, the adiabatic theory does not scale. The parameters appearing in the equation for ϵ , (IV.10), are strongly system dependent and some, α_p and C_P , are temperature dependent. To illustrate the adiabatic results in this section then, data for 3MP+NE will just be used. The equation for ϵ requires $\alpha_p, C_P, \rho_c, T_c, \frac{dT_c}{dP}$ and ξ_0^\pm , which, for 3MP+NE, can be obtained from Tables I and II.

The other parameters appearing in the theory are the universal amplitude f_1 , the cut-off α^* , and the cut-off dependent free energy parameters λ_i . As mentioned above, f_1 was set to 0.210, and in Sec. V values for the λ_i were computed for various cut-off values. What remains then is to determine an appropriate cut-off.

In isothermal decomposition, α^* is determined by requiring that it be large enough so that no unstable modes are integrated out. In the mean-field theory of Cahn,[1] the dominant unstable wavevector is at $q = \frac{1}{\sqrt{2}}$, with the largest unstable mode occurring at $q = 1$. Thus, $\alpha^* \geq 1$. While the statistical theory here gives free energy parameters that are cut-off dependent, this relation roughly holds here too.

On the other hand, the time dependent inverse susceptibility, $A(t)$, appearing in the equation of motion for

the structure factor, Eq.(III.11) does not vary with the wavevector k of the mode. In other words, the LBM ansatz produces a mean-field form for this time dependent inverse susceptibility.[6] The goal then should be to include as few concentration modes as possible into this mean-field approximation, that is, to make α^* as small as possible. A good compromise between these opposing needs is to follow LBM and just let $\alpha^* = 1$ for isothermal decomposition.

In adiabatic decomposition, the wavevector of the largest unstable mode will depend upon the degree of temperature undershoot. What has been done here is set α^* and then examine the temperature undershoot at a short time after the end of the quench, say, $\tau = 0.1$. The inverse of the equilibrium correlation length for that temperature at that time was then identified to be the minimum cut-off value, in analogy with the isothermal case. For the quenches considered here, it was found that setting $\alpha^* = 1.4$ was reasonable. For consistency, this cut-off was also used for the isothermal runs.

With the parameters in the equations determined, a quench is specified by the initial scaled temperature ϵ_i , the pressure change ΔP , and the quench time τ_{quench} . The final temperature was determined by integrating the thermodynamic function $\left(\frac{\partial \epsilon}{\partial P}\right)_S$ given in Eq. (II.34). The quench time varied with experiment, but was either known or could be deduced.

Figure 3 shows the scaled temperature, $\epsilon/|\epsilon_f|$ as a function of the scaled time τ for three adiabatic runs ending at the temperatures $T_c\epsilon_f = -0.04$ mK, -0.4 mK and -4.0 mK, with initial temperatures $\epsilon_i = -10\epsilon_f$. The quenches were on-critical so $x_0 = 0$. The scaled quench time τ_{quench} has been set to be 0.01; thus the initial temperature drop does not appear on the graph. Clearly, the temperature undershoot is large; the temperature reached immediately after the quench is roughly $-1.8|\epsilon_f|$, with the smaller final temperatures giving the greater undershoot. Note also that there is not much difference in the scaled temperature trajectories even though the final scaled temperatures differ by a factor of 100.

Figures 4 and 5 show results for the scaled peak intensity, $\tilde{S}(q_m)$, and scaled peak wavevector, q_m as functions of the scaled time τ . Results of the middle adiabatic quench in Figure 3, $T_c\epsilon_f = -0.4$ mK, are shown along with results from an isothermal run with the same ratio of $\epsilon_i/\epsilon_f = -10$. Also shown are results from an ‘‘LBM’’ version of the theory in which $\sigma(q)$, Eq.(IV.1), is set to 1 and the second term in Eq. (IV.4) due to the hydrodynamic operator \mathcal{L}_2 is dropped. Setting $\sigma(q) = 1$ assumes all modes have equilibrated, which clearly is not the case, so that value should be considered an upper bound. In Figure 4 it can be seen that the temperature undershoot causes $\tilde{S}(q_m)$ for the adiabatic quench to grow initially more rapidly than the isothermal quench.

Interestingly, $\tilde{S}(q_m)$ for the adiabatic quench in Figure 4 never differed from the peak height of the other two adiabatic quenches in Figure 3 (not shown) by more than about 5% at late times even though there is a spread

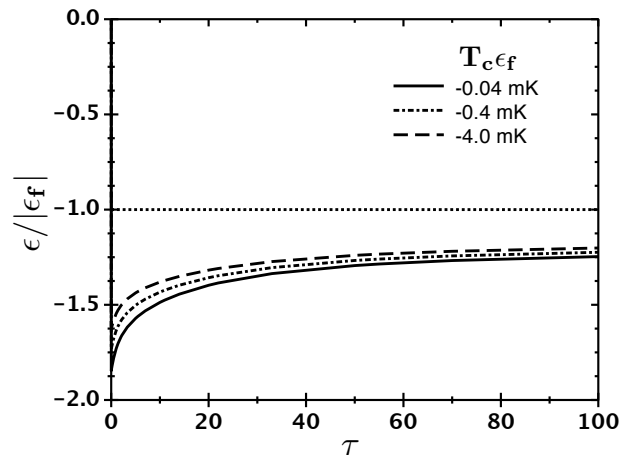


FIG. 3. Scaled temperature $\epsilon/|\epsilon_f|$ as a function of scaled time τ for three adiabatic runs. The final temperatures ΔT_f are indicated in the figure and the initial temperatures are $\epsilon_i = -10\epsilon_f$. The straight line denotes the final equilibrium temperature.

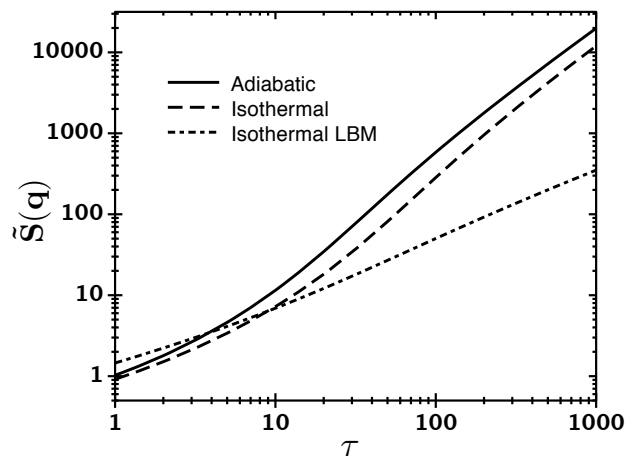


FIG. 4. Scaled structure factor peak $\tilde{S}(q_m)$ as a function of scaled time τ for an adiabatic and isothermal run of the KO theory. Also shown are predictions of an isothermal run from an LBM version of the theory. The adiabatic run is the same as the middle one in Fig.3: $\Delta T_f = -0.4$ mK and $\epsilon_i/\epsilon_f = -10$; the isothermal runs have the same ratio of initial to final temperature. Results for adiabatic runs for other temperature shown in Fig.3 gave peak values that differed at most by 5% from the $\Delta T_f = -0.4$ mK run here.

of two orders of magnitude in their final temperatures. This weak violation of scaling is caused by the weak divergence ($\alpha = 0.105$) of α_p and C_P . On the other hand, $\tilde{S}(q_m)$ for the isothermal quench differs by at least a factor of 2 from the adiabatic runs. At very early times, the LBM prediction is greater than either version of the KO theory, due presumably to the overestimation of the transport function $\sigma(q)$. At later times, LBM lags appreciably behind KO as expected.

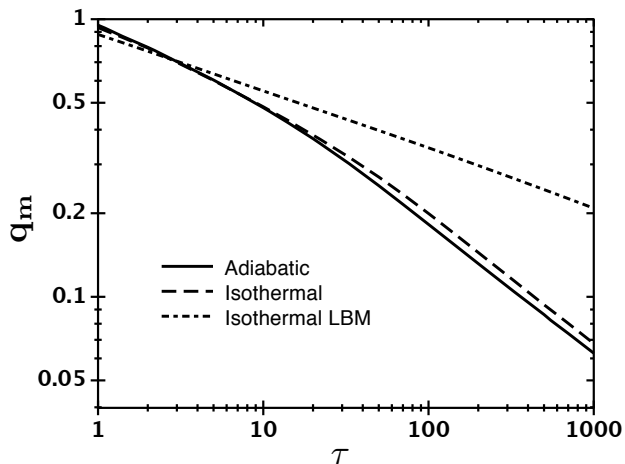


FIG. 5. Scaled peak wavevector q_m as a function of scaled time τ for an adiabatic and isothermal run of the KO theory. Also shown are predictions of an isothermal run from an LBM version of the theory. The conditions are the same as for the results shown in Fig.4. Results for the other adiabatic runs in Fig.3 were essentially identical to the one shown here.

In Figure 5 it can be seen that, surprisingly, the adiabatic and isothermal quenches give about the same value for the initial peak wavevector. This is because quenching to a lower temperature causes the fluid to coarsen at a faster rate (the characteristic decomposition time $\tau \sim \xi^3$), with eventually the adiabatic runs giving a slightly smaller q_m . Thus, one may not be able to determine any great discrepancy between the isothermal theory and experiment if one looks only at the peak wavevector.

While KO, like LBM, was created to describe the early stage of decomposition, it is interesting to examine its behavior at later times. Define time dependent exponents, a_q and a_s , so that $q_m \sim \tau^{-a_q}$ and $S(q_m) \sim \tau^{a_s}$ at any τ . For q_m , a_q increases monotonically at early times, but appears to approach a constant for $\tau > 100$. It was found that in the isothermal case KO and LBM predict that $a_q \approx 0.47$ and 0.22 , respectively, for $100 < \tau \leq 1000$. At larger times, $10^3 < \tau < 10^4$, the KO value decreases slightly to 0.46 . The exponent changed only slightly with cut-off, $a_q \approx 0.47$ and 0.46 , for $\alpha^* = 1$ and $\alpha^* = \pi/2$, respectively, for the largest times examined, $10^3 < \tau \leq 10^4$. Note that at $\tau \approx 10^4$, $q_m \approx 0.02$. In absolute terms, q_m varied less than 5% with cut-off out to $\tau = 100$.

As mentioned above, the KO theory applies to fluid flow at low Reynolds number, that is, when the viscous term in the Navier-Stokes equation is much larger than the inertial one. In this limit, it is expected that the dominant mechanism in the very late stages of coarsening yields $a_q = 1$. [41] As a consequence, the KO value for a_q can then at most be considered valid for an intermediate stage of phase separation. Interestingly though, a value of $a_q = 0.5$ has been predicted for the late stages for the opposite case of the inertial term dominating. [42]

But whether the agreement between this prediction and KO's is more than just happenstance will require more analysis.

The effective time exponent of $\tilde{S}(q_m)$, a_s , also increases at early times; however at $\tau \approx 100$ for KO it reached a maximum of 1.8 and then dropped slowly, reaching a value of 1.46 at the largest times examined, $\tau \approx 10^4$. On the other hand, experiments have shown that a_s increases monotonically with time, eventually approaching a constant. [8, 9] So this slowing in the growth of $\tilde{S}(q_m)$ seems to indicate a gradual breaking down of the theory. The peak height was more sensitive to the cut-off with the maximum of a_s for KO being 2.1 and 1.7 for $\alpha^* = 1$ and $\pi/2$, respectively. On the other hand, this maximum for KO always occurred when $q_m \approx 0.2$. (For LBM it occurs for $q_m \approx 0.35$.) This value of q_m corresponds to an average fluctuation size of $\pi\xi_f/q_m \approx 16\xi_f$. In Cahn-Hilliard theory [30], the equilibrium interface separating two phases has a width of around $4\xi_f$. Thus, at this time sharp interfaces will be forming, which the LBM and thus KO theories cannot describe. [6] At $\tau = 100$, $\tilde{S}(q_m)$ for the isothermal KO theory was 458, 285 and 239 for $\alpha^* = 1, 1.4$ and $\pi/2$, respectively, so the cut-off dependence of the theory seems to decrease as the cut-off is increased.

Scaling theory [43, 44] predicts at late times that the function $F(x) = q_m^3 \tilde{S}(q = xq_m)$ becomes constant. Interestingly, the peak of this function is almost a constant within the KO theory: $F(1) \sim \tau^{\zeta_F}$, with $\zeta_F \approx 0.07$ at late times. This trend of the theory persists at least out to $\tau \approx 10^4$.

B. Comparison With Experiment

In this section the adiabatic and isothermal theories will be compared with light scattering data of BC [11].

As stated above, in the experiments of BC the decomposition occurs adiabatically. The quenches were for on-critical mixtures so $x_0 = 0$. To compare the adiabatic theory with experiment the thermodynamic quantities, $T_c, \frac{dT_c}{dP}, \rho_c, \alpha_p, C_P$ and the two-phase values for ξ_0 and η_s , are needed. $T_c, \frac{dT_c}{dP}, \rho_c, \alpha_p$ and C_P can be found using Tables I and II. With these tables it can be deduced that $\xi_0^- = 1.13\text{\AA}$.

As mentioned above, the hydrodynamic shear viscosity, η_s , is not constant but is a singular function of ϵ . In addition, the two-phase value of η_s has not been determined, and at present there is no definite relation between the one and two-phase amplitudes. However, since the scaling form for η_s is so weakly singular and the quenches are expected to be fast, η_s was simply set equal to its one-phase value at $\xi = \xi_f$, i.e., $\eta_s \simeq \bar{\eta}(Q_0\xi_f)^{z_\eta}$, where $\bar{\eta}$, Q_0 and z_η are given in Table I.

For each quench, the initial temperature, ϵ_i , and the pressure change, ΔP , are known. The final temperature, ϵ_f , is determined by integrating $\left(\frac{\partial\epsilon}{\partial P}\right)_S$, which is given

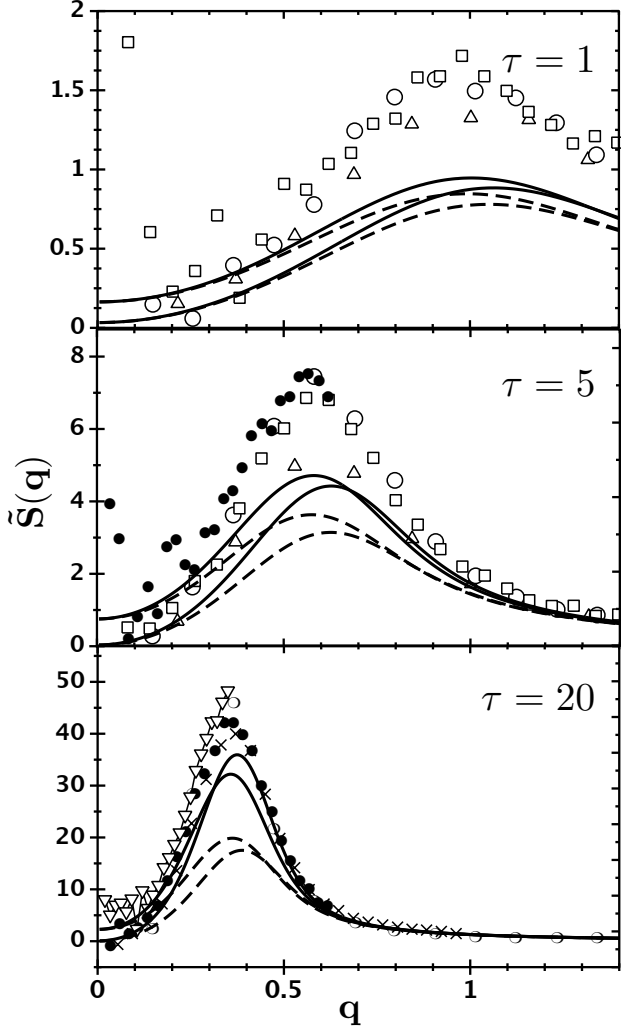


FIG. 6. Scaled structure factor $\tilde{S}(q)$ as a function of scaled wavevector q at scaled times $\tau = 1, 5$ and 20 . The initial temperature for all quenches was $T_{c\epsilon_i} = 10$ mK. The symbols denote the experimental results of Bailey and Cannell as follows: $T_{c\epsilon_f} = (\triangle)$ -0.116 mK, (\circ) -0.210 mK, (\square) -0.538 mK, (\times) -1.036 mK, (\bullet) -2.079 mK, (∇) -5.156 mK, and (\diamond) -10.37 mK. The solid and dashed curves denote results of the adiabatic and isothermal theories, respectively. For the isothermal runs for each time, the upper curve denotes results for the deepest quench shown in that time frame, while the lower one is for the shallowest. This meaning also holds for the adiabatic runs for $\tau = 1$ and 5 , but the reverse is true for the largest time, $\tau = 20$.

by Eq. (II.34). Re-evaluation of the critical properties of 3MP+NE by BC allows us to ignore any uncertainty in ϵ_f . The experimental intensity data was scaled by BC[15].

In Figures 6 and 7, the scaled structure factor $\tilde{S}(q)$ is shown as a function of the scaled wavevector q for various scaled times τ . The quenches shown all begin at $T_{c\epsilon_i} \approx 10$ mK and have final temperatures that range from $T_{c\epsilon_f} = -0.116$ mK to -10.37 mK. The solid

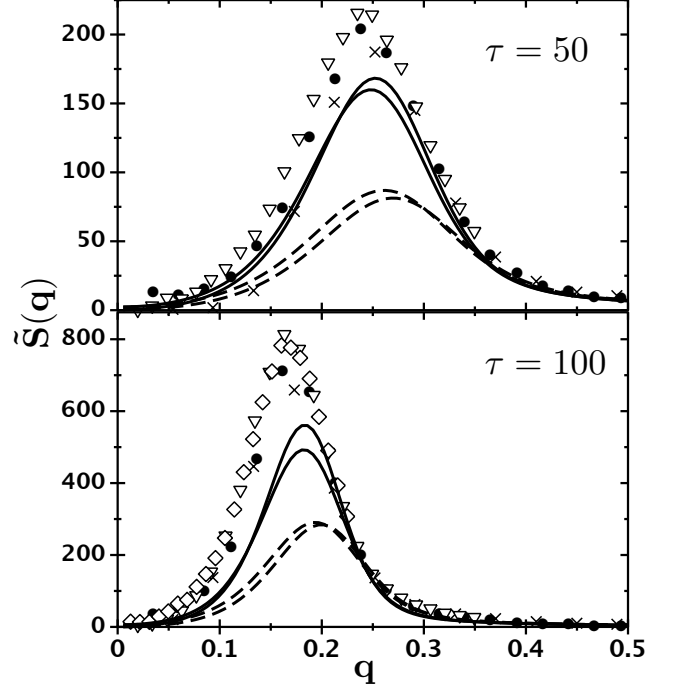


FIG. 7. Scaled structure factor $\tilde{S}(q)$ as a function of scaled wavevector q at scaled times $\tau = 50$ and 100 . The meaning of the symbols and curves and conditions are the same as in Fig.6 for $\tau = 20$.

and dashed curves denote results for the adiabatic and isothermal theories, respectively, while the points represent data of BC. For the isothermal runs for each time, the uppermost curve denotes the result for the deepest quench shown and the lower one denotes the shallowest. This meaning also holds for the adiabatics runs for $\tau = 1$ and 5 , but the reverse becomes true for larger times. The effect of a finite quench time is included in these results; the scaled quench time τ_{quench} ranged from 2×10^{-3} for the shallowest quench to 11 for the deepest.

At a very early time, $\tau = 1$, the prediction of the adiabatic theory for the peak height $\tilde{S}(q_m)$ lags behind the data by a factor of 2. However, at later times, $\tau = 20$ and 50 , the agreement with experiment is very good, within 20%. At the largest time for which data is available, $\tau = 100$, the adiabatic theory appears to start lagging behind the data again, with the difference being 30%. On the other hand, the predictions of the adiabatic theory for the peak wavevector q_m are within a few percent of the data at all times.

The LBM and thus KO theories are expected to work best at early times. For example, Mainville et al. obtained good agreement throughout the early stage, albeit with some fitting, between their experimental scattering data and the LBM theory.[7] Therefore, the disagreement between the adiabatic theory and experiment for the peak height $\tilde{S}(q_m)$ at very early times is perplex-

ing. One possibility is that setting the cut-off to a finite value removes the relaxation of high wavevector modes, $q > \alpha^*$, right after the quench. The relaxation of these modes then couple to lower q ones, increasing their relaxation, like a wave moving through q -space. To examine this hypothesis, the cut-off of the theory was varied from $\alpha^* = 1$ to $\alpha^* = \pi/2$. It was found that $\tilde{S}(q_m)$ at $\tau = 1$ varied by only 9% and 3% for the adiabatic and isothermal theories, respectively, for this cut-off range.

Another possible explanation is that the adiabatic theory has underestimated the temperature undershoot. Though whatever the cause, further research is needed.

The disagreement between theory and experiment at late times, is that at $\tau = 50$, $q_m \simeq 0.2$, which, as has been discussed above, appears to be where the KO theory begins to break down. The isothermal theory predicts a peak height and peak wavevector that lags behind experiment at all times, the difference in $\tilde{S}(q_m)$ becoming over a factor of three at the latest times.

Note that the theory results shown in Figures 6 and 7 are not quite the same as those in a previous description of the adiabatic theory, Ref.[13]. One reason is that in Ref.[13] the “double gaussian” approximation was used to solve for the time evolution of $\rho_1(y)$. As mentioned above, while this approximation is more computationally efficient than solving the full PDE for $\rho_1(y)$, Eq.(IV.6), it tends to overestimate the growth of $\tilde{S}(q)$ for times such that $q_m \geq 0.3$. Advances in computer power in the years since Ref.[13] was published have made this approximation unnecessary. A second reason is that the form for the scaled free energy density $\phi(x)$ was different in the previous work. This previous form was constructed to satisfy a constraint in the limit of the cut-off $\alpha^* \rightarrow 0$ (see Ref.[26] for a detailed description). It was subsequently concluded that the added complexity to $\phi(x)$ needed for this constraint outweighed any improved accuracy of the theory, and so here the standard “ φ^4 ” form for $\phi(x)$ was used instead.

As mentioned above, the isothermal theory predicts that if the fluid is in the critical region, the experimental data is scaled properly, and the scaled initial conditions and quench times are the same, then the scaled time evolution of any experimental run should be identical. It is interesting then whether the experimental data of BC show any violation of this scaling. Consider two experimental runs of BC with final temperatures $T_c \epsilon_f = -2.079$ mK and -0.202 mK.[15] The initial temperatures were both at $\epsilon_i \simeq 5|\epsilon_f|$ to eliminate the effect of initial conditions.[45] At $\tau = 10$, $\tilde{S}(q_m)$ was measured to be 16.6 and 18.8 for the first (-2.079 mK) and second (-0.202 mK) quench, respectively. The adiabatic theory predicts that $\tilde{S}(q_m) = 11.4$ and 12.3, for the first and second quench, respectively, while the isothermal theory predicts that $\tilde{S}(q_m) = 7.6$ and 7.7 for those quenches. Both the adiabatic and isothermal theories predict that $q_m \approx 0.47$ in agreement with both experimental runs. While the experimental violation of scaling is not large, the difference in $\tilde{S}(q_m)$ for the two runs being 12%, the

trend is in agreement with the adiabatic theory, which predicts a difference of 8%. So though there is certainly scatter in the data, this agreement at the least is suggestive evidence that the temperature change during decomposition is appreciable for this fluid.

VII. SUMMARY AND DISCUSSION

In summary, the KO-LBM theory of spinodal decomposition in binary fluids was generalized to model experimental scenarios in which the fluid is quenched by changing the pressure and the subsequent phase separation occurs adiabatically.

The central idea of the approach here was that the coarse-grained free energy, $\mathcal{F}[c]$, which governs the time evolution of the slowest modes, is constructed in a manner that creates a natural split in the degrees of freedom of the system. Those fast degrees of freedom that have been integrated out contribute to $\mathcal{F}[c]$, but also to a free energy, F_r , that is independent of the configuration $[c]$ of the slow modes. It was shown that the fast degrees of freedom, through F_r , are able to act as a thermal reservoir for the slow modes. Any global constraint though, such as constant energy or entropy, indirectly relates the state of the reservoir, and thus its temperature, to the particular state $[c]$ of the slow modes. However, it was argued that these states need be related only in an average sense. With that approximation, an equation of motion for the average reservoir temperature was derived, it playing the same role as the assumed constant global system temperature in previous isothermal theories of decomposition. The extension of the isothermal theories of KO and LBM to adiabatic conditions then consisted of: this equation of motion for the reservoir temperature; estimates for various reservoir thermodynamic derivatives, such as the heat capacity, which appear in the temperature equation; and a specification of a temperature dependent coarse-grained free energy.

This “adiabatic” theory was then applied to an on-critical mixture of 3MP+NE. It was shown that the temperature change during decomposition is appreciable and accelerates the coarsening. The adiabatic and previous isothermal theories were then compared quantitatively, with no adjustable parameters, with data of Bailey and Cannell on 3MP+NE for the structure factor at various times during the early stage of decomposition. It was shown that there is a definite lack of agreement between the data and previous theory for the structure factor peak height, and that the adiabatic theory accounts for a substantial amount of this difference. The adiabatic theory also improves the agreement with experiment for the wavevector, q_m , of the structure factor peak. Differences between theory and experiment though indicate that the adiabatic theory may still be underestimating the effects of temperature changes during decomposition for 3MP+NE. Further research is needed to determine the cause.

The large temperature change during decomposition predicted for 3MP+NE is due partly to the size of the singular term in the isobaric heat capacity compared to the background term (see Table I). Another binary fluid, isobutyric acid and water, has a much smaller singular term, and for it, at the same reduced temperatures as the Bailey and Cannell experiments, the predictions of the adiabatic and isothermal decomposition theories are essentially the same.[26] It is possible though that there are other binary fluids with even larger relative singular contributions to their heat capacity than 3MP+NE, making the adiabatic effect even more pronounced.

The adiabatic theory could possibly be extended to temperatures outside the critical region, e.g., for mixtures with longer range interactions such as polymers. However, if 3-D Ising critical scaling no longer holds, the isothermal KO/LBM theory itself becomes temperature dependent through at least the parameter f_1 (see Sec. II B). So it is unclear how the predictions of this extended adiabatic theory would differ from the near-critical one developed here, especially as thermodynamic quantities such as the heat capacity are system dependent.

The behavior of the isothermal KO theory at later times was also analyzed. It was found for times $10^2 < \tau \leq 10^4$, that q_m scaled as τ^{-a_q} , with $a_q \approx 0.46$.

While off-critical quenches were not examined here, it is expected that the adiabatic effect to be less for them since the heat released during phase separation should be largest for an on-critical mixture, it being roughly proportional to $1 - x_0^2$, using Eq. (II.43).

Interestingly, it was shown in Section II A 2 that the

entropy increase during this adiabatic decomposition is well approximated as zero. That is, in the model here, the temperature rise from phase separation exactly compensates for the temperature undershoot caused by the incomplete relaxation of the slow modes during the quench, so that the final temperature reached is as if the whole process had been reversible. In that manner, if a fluid were quenched, allowed to phase separate at least partially, and then the pressure were reversed, the fluid upon re-mixing should reach a temperature very near its initial value. A similar two-step experiment was done by Siebert and Knobler in their study of nucleation.[3, 46] While the arguments leading to this prediction of a (almost) constant entropy decomposition relied partly on the system being a near-critical binary fluid, it might be more general. Answers are left to future research.

Last, it is noted that more recent explorations of the effective temperature concept have focused on amorphous substances such as foams and glasses driven mechanically and continuously out of equilibrium.[47, 48].

ACKNOWLEDGMENTS

I thank James Langer for many helpful discussions, and Arthur Bailey and David Cannell for suggesting this problem and many discussions. I also thank John McCoy for some discussions of thermodynamic fundamentals. This work was done primarily at U.C. Santa Barbara.

-
- [1] J. W. Cahn, Trans. Metall. Soc. AIME **242**, 166 (1968).
 - [2] A. J. Bray, Adv. Phys. **43**, 357 (1994).
 - [3] A. Onuki, *Phase Transition Dynamics* (Cambridge University Press, Cambridge, UK, 2002).
 - [4] R. C. Desai and R. Kapral, *Dynamics of Self-Organized and Self-Assembled Structures* (Cambridge University Press, Cambridge, UK, 2009).
 - [5] H. E. Cook, Acta Metall. **18**, 297 (1970).
 - [6] J. S. Langer, M. Bar-on, and H. D. Miller, Phys. Rev. A **11**, 1417 (1975).
 - [7] J. Mainville, Y. S. Yang, K. R. Elder, M. Sutton, K. F. Ludwig, and G. B. Stephenson, Phys. Rev. Lett. **78**, 2787 (1997).
 - [8] Y. C. Chou and W. I. Goldberg, Phys. Rev. A **20**, 2105 (1979).
 - [9] N.-C. Wong and C. M. Knobler, J. Chem. Phys. **69**, 725 (1978).
 - [10] K. Kawasaki and T. Ohta, Prog. Theor. Phys. **59**, 362 (1978).
 - [11] A. E. Bailey and D. S. Cannell, Phys. Rev. Lett. **70**, 2110 (1993).
 - [12] The exponent z_η arises from the temperature dependence of the shear viscosity. See Table I.
 - [13] J. P. Donley and J. S. Langer, Phys. Rev. Lett. **71**, 1573 (1993).
 - [14] E. A. Clerke, J. V. Sengers, R. A. Ferrell, and J. K. Bhattacharjee, Phys. Rev. A **27**, 2140 (1983).
 - [15] A. E. Bailey, Phd dissertation, University of California, Santa Barbara, Dept. of Physics (1993).
 - [16] S. C. Greer and R. Hocken, J. Chem. Phys. **63**, 5067 (1973).
 - [17] C. M. Sorensen, Int. J. Thermophys. **3**, 365 (1982).
 - [18] H. C. Burstyn, J. V. Sengers, J. K. Bhattacharjee, and R. A. Ferrell, Phys. Rev. A **28**, 1567 (1983).
 - [19] H. Tanaka and Y. Wada, Chem. Phys. **78**, 143 (1983).
 - [20] M. E. Fisher and J.-H. Chen, J. Physique (Paris) **46**, 1645 (1985).
 - [21] A. J. Liu and M. E. Fisher, Physica A **156**, 35 (1989).
 - [22] R. B. Griffiths and J. C. Wheeler, Phys. Rev. A **2**, 1047 (1970).
 - [23] In an alternative approach, Onuki has examined the sensitivity of nucleation near the gas-liquid critical point to various types of thermodynamic constraints, including adiabatic ones, during and after a quench.[49].
 - [24] J. S. Langer, Physica **73**, 61 (1974).
 - [25] S.-K. Ma, *Modern Theory of Critical Phenomena* (Benjamin/Cummings, Reading, MA, 1976).
 - [26] J. P. Donley, Phd dissertation, University of California, Santa Barbara, Dept. of Physics (1991).
 - [27] J. S. Langer, Ann. Phys. (N.Y.) **65**, 53 (1971).

- [28] H. Callen, *Thermodynamics and an Introduction to Thermostatistics* (Wiley and Sons, U.S.A., 1985).
- [29] H. E. Stanley, *Introduction to Phase Transitions and Critical Phenomena* (Oxford University Press, New York, 1971).
- [30] J. W. Cahn and J. E. Hilliard, *J. Chem. Phys.* **28**, 258 (1958).
- [31] N. G. V. Kampen, *Stochastic Processes in Physics and Chemistry* (North-Holland, New York, 1981).
- [32] A. E. Bailey and D. S. Cannell, *Phys. Rev. E* **50**, 4853 (1994).
- [33] K. Kawasaki, *Prog. Theor. Phys.* **57**, 826 (1977).
- [34] K. Kawasaki, in *Proceedings of the Symposium on Synergetics*, edited by H. Haken (B. G. Teubner, Stuttgart, Germany, 1973).
- [35] P. C. Hohenberg and B. I. Halperin, *Rev. Mod. Phys.* **49**, 435 (1977).
- [36] W. H. Press, S. A. Teukolsky, W. T. Vetterling, and B. P. Flannery, *Numerical Recipes in C: The Art of Scientific Computing* (Cambridge University Press, NY, 1992).
- [37] www.nag.com, "Nag library of numerical routines in fortran," (1989).
- [38] C. Billotet and K. Binder, *Z. Physik B* **32**, 195 (1979).
- [39] The cause of this overshoot was investigated. It was found that it could be corrected by making the theory self-consistent, not on the second moment of the one-point probability density, but on the susceptibility. While it is possible that the kinetic version of the theory could be corrected in a similar manner, it was found not to be necessary in order to make a proper comparison with the experiments considered in this work.
- [40] A. J. Schwartz, "Calculation of hydrodynamic effects on spinodal decomposition," (1978), unpublished.
- [41] E. D. Siggia, *Phys. Rev. A* **20**, 595 (1979).
- [42] A. Sain and M. Grant, *Phys. Rev. Lett.* **95**, 255702 (2005).
- [43] K. Binder and D. Stauffer, *Phys. Rev. Lett.* **33**, 1006 (1974).
- [44] H. Furukawa, *Adv. Phys.* **34**, 703 (1985).
- [45] The times for these quenches were estimated from other data by assuming that the rate of change of the pressure was the same for all quenches.
- [46] E. D. Siebert and C. M. Knobler, *Phys. Rev. Lett.* **52**, 1133 (1984).
- [47] I. K. Ono, C. S. O'Hern, D. J. Durian, S. A. Langer, A. J. Liu, and S. R. Nagel, *Phys. Rev. Lett.* **89**, 095703 (2002).
- [48] E. Bouchbinder and J. S. Langer, *Phys. Rev. E* **80**, 031132 (2009).
- [49] A. Onuki, *Physica A* **234**, 189 (1996).